Development of Solar Array Emulator to improve Testing of Solar Products

A Dissertation

Submitted in partial fulfillment of the requirement for the award of

Degree of

Master of Engineering

In

Power Systems

Submitted By:

Ayush Munjal

Reg. no. 801241004

Under the supervision of:

Mr. Souvik Ganguli
Assistant Professor, EIED

Mr. Shripad Wachasundar
Deputy Manager, EDC

ELECTRICAL AND INSTRUMENTATION
ENGINEERING DEPARTMENT
THAPAR UNIVERSITY
PATIALA – 147004

ELECTRONICS DESIGN CENTRE
GLOBAL R&D
CROMPTON GREAVES LTD.
MUMBAI-400042

JULY 2014

DECLARATION

I hereby certify that the work which is being presented in the dissertation entitled, ***"Development of Solar Array Emulator to improve testing of solar products"***, in partial fulfillment of the requirements for the award of degree of Master of Engineering in *Power Systems* submitted in Electrical and Instrumentation Engineering Department of Thapar University, Patiala, is an authentic record of my own work carried out under the supervision of *Mr. Souvik Ganguli, Assistant Professor, EIED, Thapar University and Mr. Shripad Wachasundar, Deputy Manager, EDC, Global R&D Centre, Crompton Greaves Ltd.* and refers other researcher's work which are duly listed in the reference section.

The matter presented in the dissertation has not been submitted for award of any other degree of this or any other University.

Date: 15/07/2012

Aydsh Munjal
Reg. No. 801241004

This is to certify that the above statement made by the candidate is correct and true to the best of my knowledge.

S.P. Wachasundar

Mr. Shripad Wachasundar
Deputy Manager
Global R&D Centre, Crompton Greaves Ltd.

15/07/12

Mr. Souvik Ganguli
Assistant Professor
EIED, Thapar University

Countersigned by

(Dr. Ravinder Agarwal)
Professor & Head, EIED
Thapar University, Patiala

(Dr. S. K. Mohapatra)
Dean of Academic Affairs
Thapar University, Patiala

ACKNOWLEDEGEMENT

At the end of my dissertation, I would like to express my sincere thanks to many people who have contributed to the fulfillment of my dissertation. I want to thank my parents for their immense support and guidance. I am extremely grateful to my dissertation guides **Mr. Souvik Ganguli** and **Mr. Shripad Wachasundar**, for their valuable guidance, scholarly inputs and consistent encouragement I received throughout the dissertation work.

I also want to thank **Dr. R.S. Kaler**, Dean Resource Planning and Generation, Thapar University, Patiala for his support and guidance. And my sincere thanks to **Mr. Raja Saha, Mr. Tushar Vaidya, Mr. Hafiz Hassan, Mr. Shivkant Sharma** and my colleagues who helped me in each and every step of my dissertation so that I could complete my dissertation with positive attitude. I want to thank the HR team of Crompton Greaves for their support since the day of commencement of my training till its end.

Special thanks to all those who supported me at Crompton Greaves Ltd. (CGL) that I may have called upon for assistance, as their suggestions have helped in the development of this dissertation, generate a patent and get a recognition certificate (included in Appendix E) from CGL.

Ayush Munjal
Reg. No. 801241004

ABSTRACT

With the need for a more reliable and cost-effective technique to test the Photo-Voltaic (PV) systems, a Solar Array Emulator has been developed and the work has been presented in this dissertation to meet this concern which incorporates a configurable PV Panel/Array Simulink model that can be used to model different array configurations. It is then used to build a software module through which various PV array configurations could be created to emulate the required Solar Power, varying independently parameters of irradiance and temperature of each PV module model. This also allows us to investigate the characteristics of a PV array under different weather conditions, especially under the condition of non-uniform irradiance, and thus its' impact on the Device Under Test (DUT) can be analyzed. The PV characteristics have been achieved employing a DC/DC buck converter topology having multiple control loops with the derived model at different weather conditions. For an ideal case the outcomes are accurate to the manufacturer's datasheet curves and for a practical case the results can be compared to the actual output, hence it can be considered as an alternative to the actual PV output being used for testing and analysis of the systems. Initial programming and simulations were performed in MATLAB-Simulink, controller card schematics were made through PSPice and dsPIC programming was done in MPLAB during the development of the Solar Array Emulator.

TABLE OF CONTENTS

LIST OF APPENDICES

LIST OF FIGURES

LIST OF TABLES

List of Abbreviations

SAE	Solar Array Emulator
NREL	National Renewable Energy Laboratory
MNRE	Ministry of New and Renewable Energy
PV	Photo-Voltaic
OC	Open Circuit
SC	Short Circuit
MPP	Maximum Power Point
MPPT	Maximum Power Point Tracker
STC	Standard Test Condition
DUT	Device Under Test
DC/DC	Direct Current/Direct Current
PWM	Pulse Width Modulation
PIC	Programmable Interface Circuit
IC	Integrated Circuit
PCB	Print Circuit Board
KVL	Kirchoffs Voltage Law
KCL	Kirchoffs Current Law

Chapter 1

1 Introduction

In recent decades, there has been a spurt in the demand of energy leading to fossil fuel consumption surge, causing high levels of environmental pollution. Also the increasing gap between supply and demand of energy has resulted into a spurt in the use of renewable sources of energy; making it a hot topic for researchers [1-3]. Since, Photo-Voltaic (PV) power generating systems are more advantageous among all the renewable resources; zero emissions while generating electricity make them environmentally friendly. Due to the abundant availability of the discussed resource, it is the most secure of all sources.

India being located in the equatorial Sun Belt is endued with rich solar energy resource. Theoretically, India's solar power reception energy is of about 5000trillion kWh/year with about 300 clear sunny days in a year and with most parts of the region receiving 4-7 kWh/m^2/day [4-5]. Figure1 shows the annual average of direct normal irradiance for the Indian region from National Renewable Energy Laboratory (NREL). Theoretically, entire country's solar power requirement can be met by effective capture of just a small fraction of the total incident solar energy and thus it is being widely employed in many applications. It is also clear that every effort needs to be made to exploit the relative abundant sources of energy available to large proportion of poor and energy unserved population in the country. This quest for power utilization has been analyzed by the Ministry of New and Renewable Energy (MNRE) which unveiled in 2009 a $19 billion plan to produce 20GW of solar power by 2022 under the Jawaharlal Nehru National Solar Mission (JNNSM) [6].

Thus, with a life expectancy of 25-30yrs[7], PV system finds application not only at the commercial level but also in residential power systems, including the off-grid decentralized applications which find a greater role from rural electrification prospective. Also highly efficient and expensive solar cells are being developed and used to support power requirements of satellites and other space missions. With the increasing global presence of Indian Space research, the solar power driven satellites and the future of space solar plants along with all the domestic and commercial need largely motivates the use of solar technology in India and thus can be harnessed effectively providing a huge scalability for solar power generation.

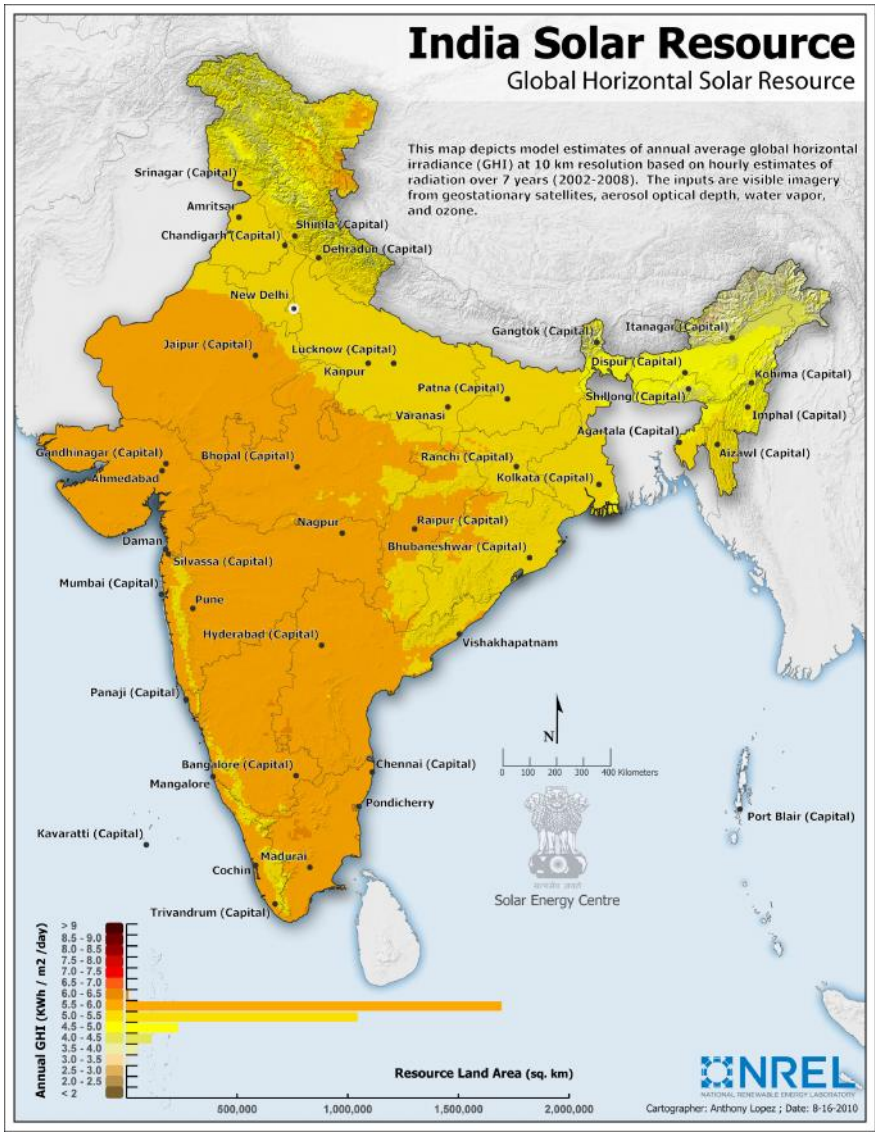

Figure1 Annual average of direct normal Irradiance for the Indian region [8]

All the solar dependent equipments are needed to be tested and analyzed before they go for field installation. Also the trend moves toward higher power solar panel arrays and more efficient solar inverters and Maximum Power Point Tracking (MPPT) chargers. Further, there is a need for an alternate secondary power source to PV panels, a specialized DC power source, for testing and validation purpose that is more reliable, repeatable, scalable, cost effective, and available off the shelf. Designers of micro-inverter, solar pump, solar refrigerator, space research experts and designers of varied solar based applications need to verify accuracy and efficiency of their algorithms and equipments to gain competitive advantage in the market. To meet these requirements the concept of Solar Array Emulator (SAE) comer forward. It comes into picture when we look to setup a testing bed for such equipments.

The main goal of this dissertation is to study and develop a SAE to meet the need of testing and validation of solar power based application products at various irradiance and temperature level. Study has been supported by simulations of the PV panel model and the combined system with DC/DC Buck converter has been performed in MATLAB Simulink and the implementation of the same has been done using Microchip's dsPIC30F controller with Embedded C based programming in MPLAB software.

1.1 Overview of PV panels and arrays

Conventionally, PV systems include PV arrays and power converters. An array is formed by a series-parallel combination of solar modules or panels. The output of this power source depends on some external factors majorly categorized into natural and installation factors. Natural factors include incident light intensity or irradiance (G) on the panels, ambient temperature. Installation factors linked with the panels include tilt angle, orientation angle with respect to true south, and unavoidable shading of the modules.

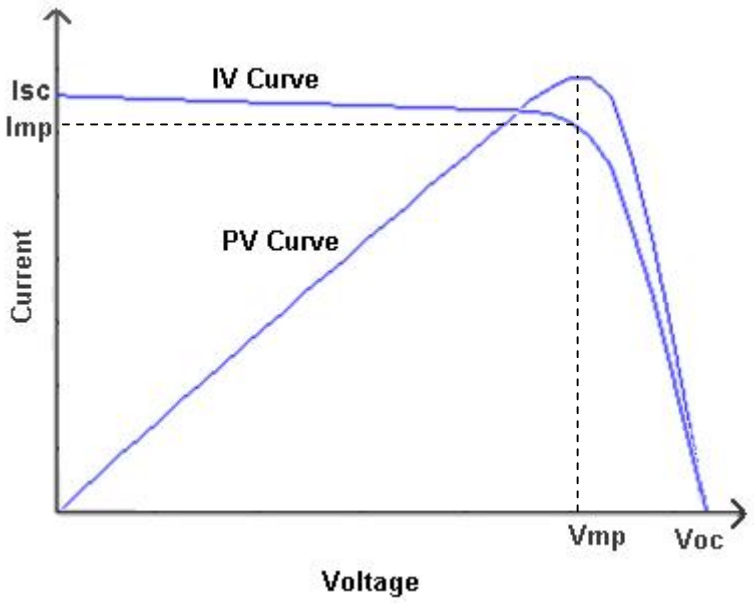

Figure2 Ideal IV and PV Curve for a solar panel

The most known parameters of the photovoltaic panel as mentioned in the manufacturer's datasheet are the Open Circuit Voltage (V_{OC}), Short Circuit Current (I_{SC}), Maximum Power Voltage (V_{MP}), and Maximum Power Current (I_{MP}). Apart from the mentioned parameters few other parameters which play crucial role in PV modeling are Nominal Operating Cell Temperature (NOCT), temperature coefficients for voltage, current and power (K_V, K_I, K_P) [9]. These values define the points of the I-V characteristics of the panel. Figure2 shows ideal IV and PV Curves for a solar panel.

Two of the problems that still affect the performance and reliability of photovoltaic modules are shading and mismatch. Shading occurs when PV systems have been installed in locations where some exposure to shading is inevitable such as in circumstances where there is not enough land available to build a PV installation to prevent all types of shading. Shading of PV cells may also occur in situations such as leaves, bird droppings on PV cells, or by shadow casting over the PV cells. The problem with shading is that it can significantly reduce the power output of a PV array and output characteristics will be more complicated. Bypass diodes are commonly used in PV arrays to protect against the effects of shading by limiting the effects of power loss and hot-spot power dissipation [10-11].

1.2 Motivation and Objectives

Development of SAE is needed for testing, validation and analysis of solar products and equipments. Lab testing, through PV panels test setup would not only be cumbersome, bulky, space-consuming, but most importantly costly and time consuming. It will be very time consuming due to the solar dependency which might be unavailable for extended period of time and thus making the project cost ineffective. Thus we need an alternate power source like SAE to test our systems, which would eradicate the need of PV panels for testing and validation purposes.

Emulator to be made should be reliable, repeatable, scalable, cost effective, and available off the shelf. Thus it would characterize the behavior of solar applications at a fraction of the cost of an actual cell/panel/array. The benefits and features for developing the SAE are as follows:

- Reliable - Eliminates the need of PV panels and arrays.
- Flexible - Different types of Panel at different weather conditions can be emulated.
- Availability - Allows Continuous testing (Not dependent on day & night).
- Redundant performance.
- Convenient & User friendly.
- Safety – Proven CG system ensures safety of its customers and DUT.

1.3 Outline of Dissertation

Chapter 2 focuses on the literature review of papers related to the work including PV modeling, solar emulators, designing and analysis of dc-dc converters.

Chapter 3 discusses about various parts of SAE from modeling of PV model with single diode model which further stretches the effect of change in weather conditions namely irradiance and temperature on the model, MPPT concept.

Chapter 4 describes the methodology, implementation of software with the help of flow charts and implementation of hardware using PSpice schematics along with the design calculations for DC/DC Buck converter topology. Section has been explained with well defined block diagrams.

Chapter 5 sums up the dissertation work along with future scope.

Chapter 2

2 Literature Survey

2.1 Introduction

In this chapter, review of the literature is done which provides a deep insight of the technology aspects of Solar PV cell modeling, Solar Simulators designing concepts and power converter designing with the current state of the art research and development in this field.

2.2 Literature Review

Vokas *et al.* [12] presented a derivation of the characteristic measurements of a PV cell using computer modeling. This computer simulation program was able to compute the light current, short circuit current, open circuit voltage and efficiency of the cell at different operating temperature.

Lloyd *et al.* [13] proposed the design and construction of a modular electronic PV simulator. The simulator was modeled using Ispice and Simulink. To obtain an optimal compromise between accuracy and dynamic performance for the controller a linearised model was derived.

Veerachary *et al.* [14] developed a MPPT algorithm using only solar cell array voltage information. This helps in obtaining current sensorless tracking control. An improved converter system was proposed to overcome the inadequacy of a boost converter for the voltage based MPP control. The proposed system resulted in low ripple content, resulting into lower value of capacitance and improved array performance.

Veerachary *et al.* [15] presented a simple and accurate PV model suitable for PSIM based circuit-oriented simulator. The model was verified by generating I-V characteristics through simulation for different solar insolations and then compared with characteristics obtained experimentally. The PV system was integrated with developed circuit models and as an example MPPT of PV system with dc/dc converter was considered.

Sera *et al.* [16] presented an approach for construction of a model for a PV panel employing single-diode five-parameter model, based exclusively on data-sheet parameters. The model considered series and parallel resistance of the panel. The PV panel model was able to predict the panel behavior at different temperature and irradiance conditions.

Midtgard *et al.* [17] developed a PSpice computer model for a PV panel including the effects of bypass diodes and partial shading. The PV module characteristics obtained from real-life measurements has been used to deduce the PV model. A modification of the signal side load had also been presented to develop a prototype for testing.

Cirrincione *et al.* [18] presented a DC/DC buck converter circuit for real-time laboratory simulation of renewable sources. The converter described the current-voltage characteristic of a PV array and of a fuel cell (FC). The converter was able to reproduce the electrical characteristics of experimental generator both in the steady state and transient conditions. The effectiveness of the proposed circuit was verified by the laboratory experiments, obtained by implementing the converter control on a low cost digital signal processor (DSP) board.

Yuan *et al.* [19] formulated a hybrid control strategy for a PV simulator, which emulated the output characteristics of PV arrays under different loads, temperature and irradiation. The mathematic modeling of the I-V curve of PV arrays was investigated in this paper and accordingly the current control or voltage control method was carried out for different segments of PV output characteristics. The control unit was based on TMS320LF2407 DSP which calculated and controlled the current or voltage respectively.

Koran *et al.* [20] presented a systematic design technique for a PV simulator. The proposed technique aided in improving control loop bandwidth and system response. The PV equivalent circuit was used to generate current-voltage reference curves. A novel technique was proposed and implemented with analog controllers. A two-stage LC output filter was implemented to push the resonant frequency higher, thus allowing a higher bandwidth control loop design keeping the same switching ripple attenuation as in the conventional one-stage LC output filter.

Hengsi *et al.* [21] proposed an approach to extract equivalent circuit parameters of PV Cells. Particle swarm optimization (PSO) was applied to extract the solar cell parameters. The proposed approach obtained good parameter precision under the variation of temperature and solar insolation.

Wandhare *et al.* [22] proposed a compact, cost effective photovoltaic emulator. The emulation of current-voltage characteristics of the PV source is achieved for varying solar radiation and temperature. The proposed system accommodated the re-configuration of PV panels for series and parallel connection. The system was implemented using a low end dsPIC microcontroller and the hardware prototype uses a flyback converter topology to achieve a power of 150W.

Ickilli *et al.* [23] developed a PV emulator system based on a dc/dc converter. The model could handle dependence of all parameters in PV model with respect to temperature and solar irradiation. The proposed emulator system was controlled by an Altera Cyclone-III FPGA development board. Experimental results showed that the output characteristics of the PV emulator were in accordance in with the actual PV panel output.

Bhise *et al.* [24] presented a scheme to generate PV characteristics for any desired environmental conditions with the help of programmable power supplies using the National Instrument's LabVIEW platform. The proposed system could emulate PV modules under different temperature, illumination levels and with different shading patterns.

Chen *et al.* [25] developed a DSP based programmable emulator for the photo voltaic panels. A solar illumination model including the partial shading effect had also been proposed. The model could be programmed for different temperatures. The effect of dust and solar oblique incidence had also been taken into consideration. The emulator has been realized using buck converter topology with rectified AC input.

Lu *et al.* [26] proposed use of piecewise linear approach in modeling of PV characteristics for PV emulator for easier implementation in a low-cost micro-controller. It was further then used to develop the hardware prototype of the same using a buck-boost converter topology. The system was also tested using resistive load and maximum power point tracker.

Kim *et al.* [27] developed a dual mode power regulator, i.e. current regulator and voltage regulator, for PV emulation. The complementary use of two regulators was done for power hybridization. The proposed emulator results showed accurate operation over the full operating range of the PV module.

2.3 Conclusion

From the literature review it is found that not only piecewise linear approach but artificial intelligence techniques like PSO have been used in parameter estimation of PV model. This has then been integrated into the hardware prototype with different power topologies like flyback, buck, and buck-boost converters to achieve PV emulation. In the subsequent chapter we will discuss about the PV modeling and commonly used MPPT techniques.

Chapter 3

3 PV modeling and MPPT

3.1 Introduction

In order to understand the working of SAE, a thorough understanding of the modeling of Solar PV panels and implemented MPPT techniques is required. In this chapter, the concepts of PV modeling and types of MPPT techniques along with their advantages and disadvantages have been discussed.

3.2 PV Modeling

Solar panels are one of the essential parts of a PV system which convert solar energy to electrical energy and have nonlinear I-V characteristic curves. Accurate prediction of the system electrical behavior needs to have comprehensive and precise models. Consequently, it provides a valuable tool in order to investigate the electrical behavior of the solar cell. In the literature, models that used to express electrical behavior of a solar cell are mostly one-diode or two-diode models with a specific accuracy with respect to each other. One-diode model is described with five variable parameters while the two-diode model with seven variable parameters in different environmental conditions, thereby increasing the complexity of the system.

3.2.1 Mathematical Expression of a Solar Cell

3.2.1.1 Two-diode Model

In this model, the solar cell is modeled as a current source connected in parallel with a rectifying diode. However, in practice the current source is also shunted by another diode that models the space charge recombination current and a shunt leakage resistor to account for the partial short circuit current path near the cell's edges due to semiconductor impurities and non-idealities. In addition, the solar cell metal contacts and the semiconductor material bulk resistance are represented by a resistor connected in series with the cell shunt elements [27-28]. The equivalent circuit for this model is shown in Fig. 1.

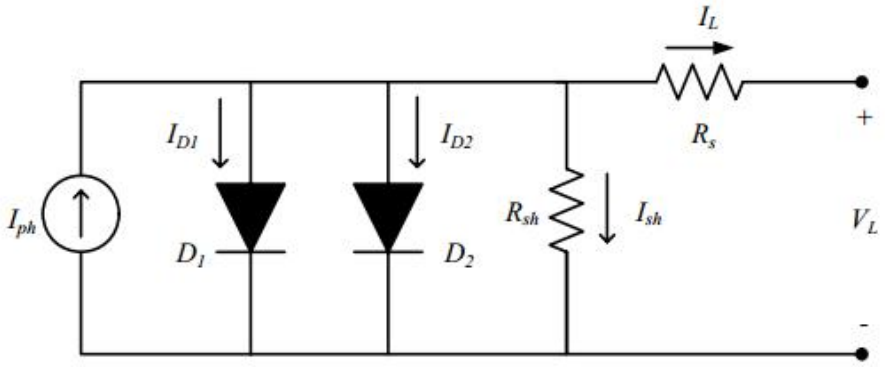

Figure3 Equivalent circuit of a double diode model

In this double-diode model, the cell terminal current is calculated as follows:

$$I = I_{ph} - I_{D1} - I_{D2} - I_{sh} \tag{3.1}$$

where,

I_L : Terminal Current

I_{ph} : Cell-generated photocurrent.

I_{D1}, I_{D2} : First & second diode currents

I_{sh} : Shunt resistor current.

Shockley equation is used to express the two diode currents while the leakage resistor current I_{sh} is formulated as shown below,

$$I_{D1} = I_{SD1}\left[\exp\left(\frac{V + I \times R_s}{A_1 \times V_T}\right) - 1\right] \tag{3.2}$$

$$I_{D2} = I_{SD2}\left[\exp\left(\frac{V + I \times R_s}{A_2 \times V_T}\right) - 1\right] \tag{3.3}$$

$$where\ , V_T = \frac{Kq}{Tc}$$

$$I_{sh} = \frac{V_{sh} + I \times R_s}{R_{sh}} \tag{3.4}$$

where R_s and R_{sh} are the series and shunt resistances respectively; I_{SD1} and I_{SD2} are the diffusion and saturation currents respectively; V_L is the terminal voltage; n_1 and n_2 are the diffusion and recombination diode ideality factors; k is Boltzmann's constant; q is the electronic charge and T is the cell absolute temperature in absolute scale. Substituting these equations into the cell terminal current is now rewritten as shown below,

$$I = I_{ph} - I_{SD1}\left[\exp\left(\frac{V + I \times R_s}{36 \times A_1 \times V_T}\right) - 1\right] - I_{SD2}\left[\exp\left(\frac{V + I \times R_s}{36 \times A_2 \times V_T}\right) - 1\right] - \left[\frac{V + I \times R_S}{R_{sh}}\right] \quad (3.5)$$

The I-V characteristics are fully described by seven parameters i.e. R_s, R_{sh}, I_g, I_{SD1}, I_{SD2}, n_1 and n_2.

3.2.1.2 Single Diode Model

In this model, the basic single diode model has been realized concluding the effects of irradiance and temperature [29]. Its equivalent circuit with series and parallel resistance is shown in Figure4.

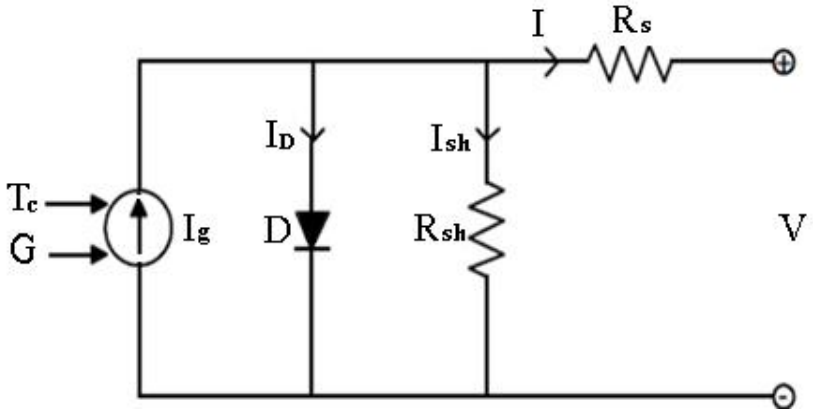

Figure4 Single Diode model based Equivalent circuit of a single solar cell

The symbols in Figure4 are defined as follows:

Ig : Photo-current or generated current;

I_D : Diode current;

I_{sh} : Shunt current;

I : Output PV (panel) current;

V : Output PV (panel) voltage;

D : Parallel diode;

R_{sh} : Shunt resistance;

R_s : Series resistance;

G : Irradiance;

Tc : Cell Temperature;

V_{sh}: Shunt Resistance Voltage drop;

V_D : Voltage across the diode.

The IV equation for Figure4 is expressed as

$$I = I_g - I_D - I_{sh} \tag{3.6}$$

$$I_D = I_o\left[\exp\left(\frac{V + I \times R_s}{A \times V_T}\right) - 1\right] \tag{3.7}$$

$$I_{sh} = \frac{V_{sh}}{R_{sh}} \tag{3.8}$$

$$V_D = V_{sh} = V + I \times R_s \tag{3.9}$$

where,

Io : Reverse saturation current of the diode,

A : Curve fitting factor.

q : Electron charge (1.602 × 10-19C),

K : Boltzmann constant (1.38 × 10-23 J/K).

3.2.2 Model of a PV module

There are many equivalent circuits of a solar cell, where the single-diode and two-diode models can be most widely used. Since the single-diode model is simple and accurate enough in many cases [30], it is applied in modeling of the panels. In single-diode model, there is a current source parallel to a diode. The current source represents light-generated current I_g that varies linearly with solar irradiation. This is the simplest and most widely used model as it offers a good compromise between simplicity and accuracy. A more practical model can be seen in figure4, where R_s represents the equivalent series resistance and R_{sh} the parallel resistance. Based on the above equivalent circuit of a photovoltaic panel, its characteristic equation is deduced as,

$$Since\ , R_s << R_{sh} \tag{3.10}$$

$$thus\ , V_{sh} \approx V \tag{3.11}$$

$$I = I_g - I_o\left[\exp\left(\frac{V + I \times R_s}{36 \times A \times V_T}\right) - 1\right] - \frac{V}{R_{sh}} \tag{3.12}$$

3.2.3 Model of a PV array

A PV array is a group of PV modules which are electrically connected in series-parallel configuration to produce required high power for specific current and voltage [33-34]. The equivalent circuit for the solar module arranged in parallel and series is shown in Figure5. In fact, the PV efficiency is sensitive to small change in R_s but insensitive to variation in R_{sh}.

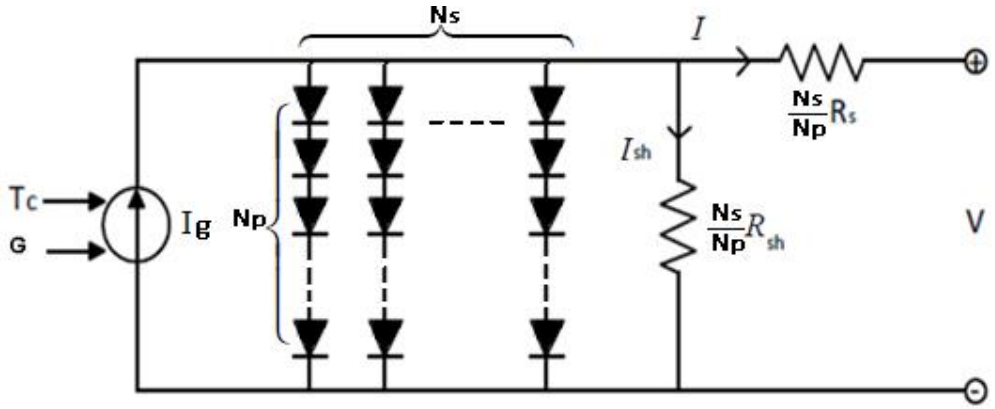

Figure5 Equivalent Circuit of PV Array by extending the single diode model.

The symbols in Figure5 are defined as follows

N_S= Series connected number of modules.

N_P= Parallel connected number of set of modules.

An appropriate equivalent circuit for all PV module (36 cells), and array is generalized. The equation for terminal current and voltage of the array is [31, 32].

$$I = I_g - N_p \times I_o \left[\exp\left(\frac{\frac{V}{N_s} + \frac{I \times R_s}{N_p}}{36 \times A \times V_T} \right) - 1 \right] - \frac{V \times N_s / N_p + I \times R_s}{R_{sh}} \quad (3.13)$$

3.2.4 Irradiance and Temperature dependence

Output of the I-V characteristic equation of the derived PV model is affected by changes in irradiance level and cell temperature of the PV module. These effects can be modeled by set of equations described as follows:

$$I_{sc(Tc,G)} = \left[I_{sc} + \sim_i \times (T_c - T_{stc}) \right] \times \frac{G}{G_{stc}} \quad (3.14)$$

where, G_{stc} and T_{stc} are the light-generated current and cell temperature of the module respectively at Standard Test Conditions (STC). The diode saturation current dependence and the open circuit voltage dependence on temperature can be expressed by:

$$I_o = I_{rs} \left(\frac{T_c}{T_{stc}} \right)^3 \exp \left[\frac{qE_g}{AK} \left(\frac{1}{T_c} - \frac{1}{T_{stc}} \right) \right] \qquad (3.15)$$

$$I_{rs} = \frac{I_{sc,r}}{\exp \left[\frac{qV_{oc}}{AKT_{stc}} - 1 \right]} \qquad (3.16)$$

$$V_{oc,Tc} = V_{oc} + \sim_v \times (T_c - T_{stc}) \qquad (3.17)$$

where,

E_g : Band-gap energy of semiconductor,
(Eg=1.12eV for the polycrystalline Silicon at 25°C)

I_{rs} : Reverse saturation current of the diode at STC.

$\sim_i$: Current Temperature Coefficient.

$\sim_v$: Voltage Temperature Coefficient.

The module is operated best at a Normal Operating Cell Temperature (NOCT) of 33°C, the worst at 58°C and typical module at 48°C respectively. An approximate expression for calculating the cell temperature is given by:

$$T_c = T_a + \frac{NOCT - 20}{80} \times G \qquad (3.18)$$

3.3 Maximum Power Point Tracking (MPPT)

MPPT tracking algorithm is responsible for drawing maximum power out of the solar cells at different environmental conditions. Since SAE would be responsible in analyzing the Device Under Test (DUT) like MPPT charger, it is necessary to have a clear knowledge about the MPPT concept and related algorithms. Various MPPT algorithms have been stated in the literature. A comparison between them is show in Figure6 on the basis of tracking factor. Few of the most cited MPPT algorithms are as follows:

- Fixed Duty Ratio
- Hill Climbing
- Perturb & Observe
- Incremental Conductance
- Constant Voltage

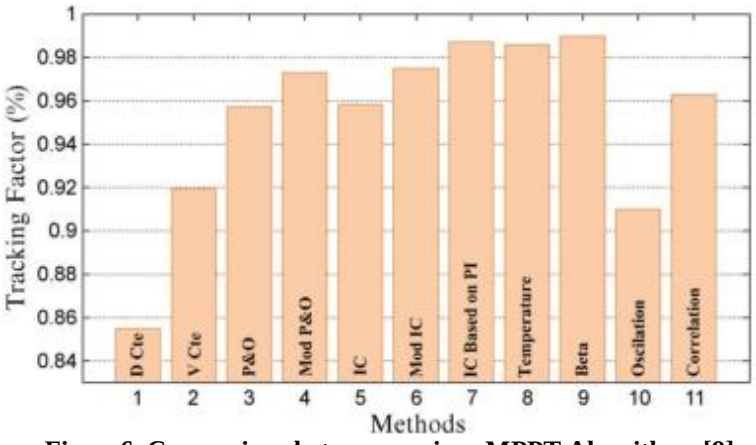

Figure6 Comparison between various MPPT Algorithms [9]

3.3.1 Fixed Duty Ratio

The fixed duty cycle represents the simplest of the methods, and it does not require any feedback, where the load impedance is adjusted only once for the MPP. This method is not an efficient one since it doesn't track the changing the MPP with respect to the changing environment conditions like temperature and irradiance.

3.3.2 Constant Voltage (CV)

The CV method uses empirical results, indicating that the voltage at MPP is around 70%–80% of the PV V_{OC}, for the standard atmospheric condition. Among the points of MPP, at varying environmental conditions, the terminal voltage of the module varies very little with respect to the changes in intensity of solar radiation, but it varies when the changes in temperature. Thus, this method must be used in regions where the variation in temperature is very little. This method provides the advantage of simple implementation since only PV voltage is required and a simple control loop can help reach the MPP.

3.3.3 Perturb and Observe (P&O)

The P&O method operates by incrementing or decrementing the output terminal voltage of the PV cell in a periodical manner and thereby comparing the power obtained in the current cycle with the power of the previous one, thus performing dP/dV. If the power increases with increase in voltage then the control system changes the operating point in that direction. Otherwise, the operating point is changed in the opposite direction. The voltage is varied at a constant rate, only when the direction for the change of voltage is known. To allow the balance between faster response and less fluctuation in steady state this rate as a parameter should be adjusted. A modified version is obtained when the steps are changed according to

the distance of the MPP and thus resulting into higher efficiency. This method is more generic and thus an excellent method to reach the MPP. However, this method may suffer from the fast changes in environmental conditions of irradiance and temperature.

3.3.4 Incremental Conductance (IC)

The IC method is based on the fact that the power slope of the PV is null at MPP (dP/dV=0), positive in the left and negative in the right, as shown in Figure 2. Thus due to this condition the MPP can be found in terms of the increment in the array conductance. Using the following equation, it is possible to find the IC conditions. Theoretically, steady-state oscillations should be eliminated once the derivative of power with respect to voltage is null at MPP. However, null value of this slope hardly ever occurs due to the digital implementation resolution. One of the strong point is that this method does not suffer from fast transients in environmental conditions. The IC method needs to monitor both the current and voltage of the PV as in P&O method. However, it is not necessary to calculate the PV power.

$$\frac{dp}{dv} = \frac{d(v \times i)}{dv} = i + v.\frac{di}{dv} = 0 \qquad (3.19)$$

$$\frac{\Delta i}{\Delta v} = -\frac{i}{v} \quad (a)$$

$$\frac{\Delta i}{\Delta v} > \frac{i}{v} \quad (b)$$

$$\frac{\Delta i}{\Delta v} < \frac{i}{v} \quad (c)$$

where, (a)condition at MPP, (b)condition to the left of MPP, and (c)condition to the right of MPP.

3.4 Conclusion

In this chapter we discussed the modeling of PV cells, panels and arrays and most cited MPPT techniques to gain an understanding of the basics of models employed in SAE and the algorithms it is suppose to test and validate. In the subsequent chapter we will be having a detailed SAE system description.

Chapter 4

4 System Description

4.1 Introduction

SAE system comprises of two subsystems, each with its own features. The two subsystems are namely the Converter Unit, and Control Unit. These subsystems are connected in accordance with the block diagram presented in Figure3. The block diagram explicitly details the functioning of the system.

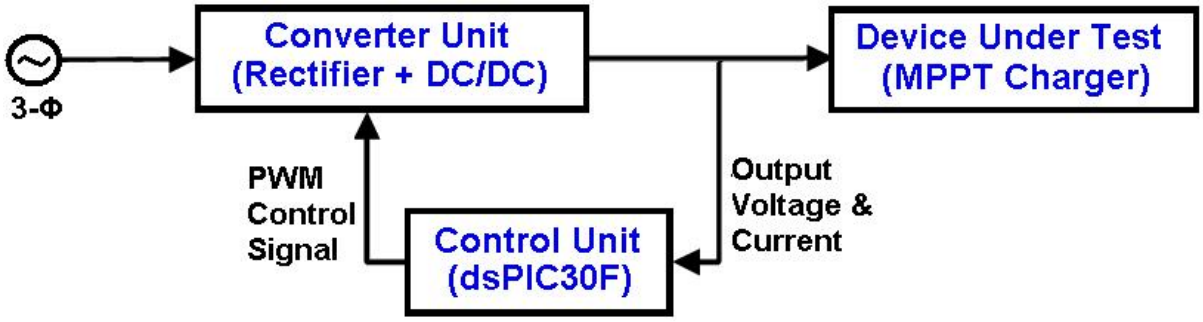

Figure7 System Block Diagram

The first subsystem, i.e. the converter unit consists of a 3-Phase Rectifier whose output is connected to the input capacitor filters of DC/DC Buck converter. These input capacitors ensure a steady DC input to the buck converter. The buck converter is controlled by a PWM signal which is responsible for maintaining the programmed output voltage and current in accordance with the selected PV Panel configuration. Output of the converter is again filtered out by the two parallel output capacitors in quest to achieve a fine DC output.

The second and most important subsystem is the Control Unit, which includes the programmed PV panel model responsible for producing the reference in accordance to the IV characteristics of the panel within the dsPIC30F5013. This reference is then used to generate PWM signal through IC SG3524 with feedback from the emulator Inductor current sensor, which is then fed to the IGBT gate driver IC MC33153 to complete the control operation.

In the subsections we will be discussing about the employed modeling of PV panel and array, followed by a detailed discussion of the control system involved in SAE, explicitly explained with block diagrams and PSpice schematics, and then a detailed discussion with Simulink model for the combined converter and control unit.

4.2 Employed PV Configuration

With the use of equations (3.1-3.13), Figure8 shows a generic mathematical Simulink model for PV panels requiring all the datasheet parameters which has then been deduced for 130W panel (WS-130) of WAAREE make. The model is used to obtain the desired ideal I-V characteristic, as shown in Figure2 and I-V characteristics for different Irradiance (G) and cell temperature (Tc).

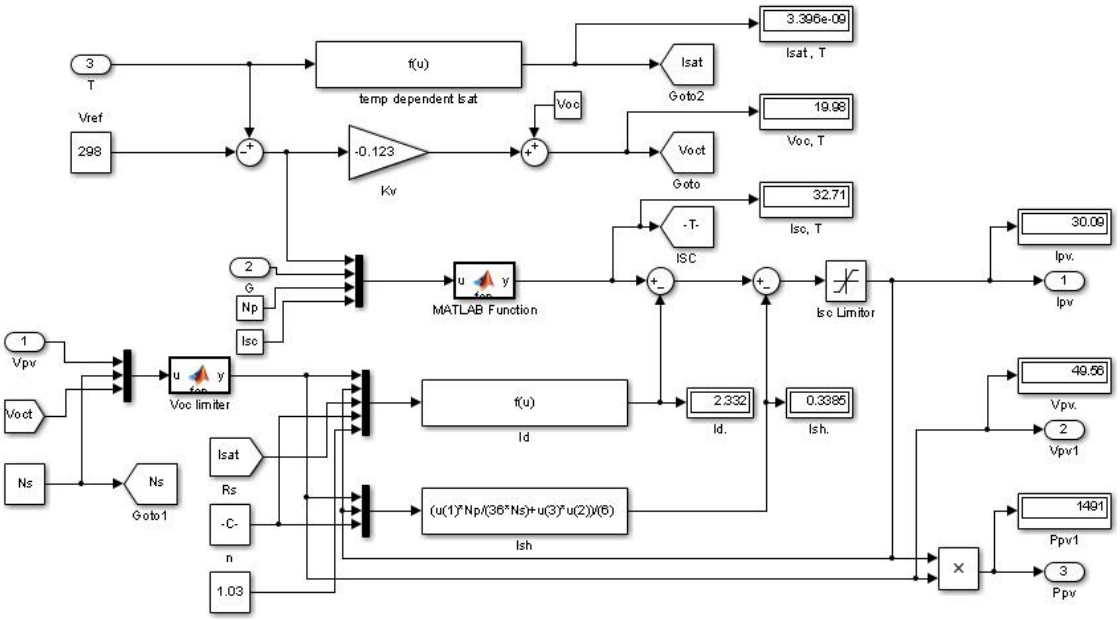

Figure8 Simulink Model of the derived PV panel model

Specification of the mentioned PV panel is shown in Table I., datasheet included in Appendix B, which has been used in the PV panel modeling of the system. Using which, SAE is configured to realize a solar array of 3x4 panel configuration i.e. 3 panels in series and 4 such sets in parallel. The resulting system specification is shown in Table II. To digitally implement the emulation of PV array through hardware, the PV equivalent circuit replaced with the derived equations (3.8-3.13) has to be converted into an embedded C based code. This code is then written into Microchip's dsPIC30F5013 through the interfacing software and kit involving MPLAB and ICD3 respectively. The model uses a straight mathematic input-output relation to make the emulator resemble the actual solar cell.

From the point of its implementation, the algebraic loop formed in model equation (3.8) due to the input parameter I is removed by adding a delay in the loop through ADC interrupt cycle of dsPIC30F. So in the digital implementation of the equation the input I to the equation is nothing but I (Iref) calculated in the previous cycle. And the input V to the model equation (3.8) is taken as the load voltage or the drop across the load or output capacitor

voltage. Another modification is based on the assumption that the generating current is equal to the short-circuit current. The modified digital model reference equation can be re-written as:

$$I_{ref} \text{ or } I\{n) = I_{sc} - N_p \times I_o \left[\exp\left(\frac{\frac{V_o}{N_s} + \frac{I_{(n-1)} \times R_s}{N_p}}{36 \times A \times V_T} \right) - 1 \right] - \frac{V_o \times N_s / N_p + I_{(n-1)} \times R_s}{R_{sh}} \quad (4.1)$$

Table I Datasheet value of WAAREE WS-130

PV Module Specification	
Parameters	**Values**
Open Circuit Voltage (Voc)	21.00 V
Short Circuit Current (Isc)	8.25 A
Maximum Power Voltage (Vmp)	17.00 V
Maximum Power Current (Imp)	7.65 A
Maximum Power (Pmp)	130.00 W

Table II Net system configuration (3x4)

PV Array Configuration	
Parameters	**Values**
Open Circuit Voltage (Voc)	63.00 V
Short Circuit Current (Isc)	33.00 A
Maximum Power Voltage (Vmp)	51.00 V
Maximum Power Current (Imp)	30.60 A
Maximum Power (Pmp)	1560.00 W

4.3 Control System

SAE is realized using an IGBT based buck converter with PI controller and PWM generator. With 3-Φ rectified input, buck converter is current controlled to regulate the power switch. The designed circuit is a current controlled voltage source. Output current is controlled by comparing it with the reference (I_{ref}) determined by the PV model, whose inputs have been discussed in the previous sections. SAE block diagram is shown in Figure9.

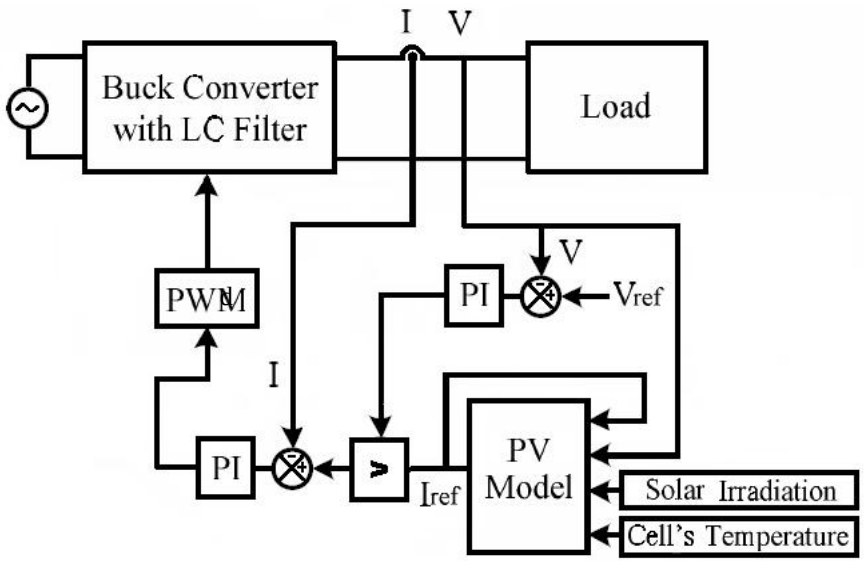

Figure9 Block diagram of Solar Array Emulator

The control block diagram in Figure10 shows two control loops, i.e. voltage control loop or current control loop. Dominance of one of the loop is dependent upon the set priority. Priority for voltage loop is more than the current loop under no-load operating condition and voltage limiting condition (Voc) depending upon the selected array configuration. And under normal operation and short circuit conditions the priority of current loop is more.

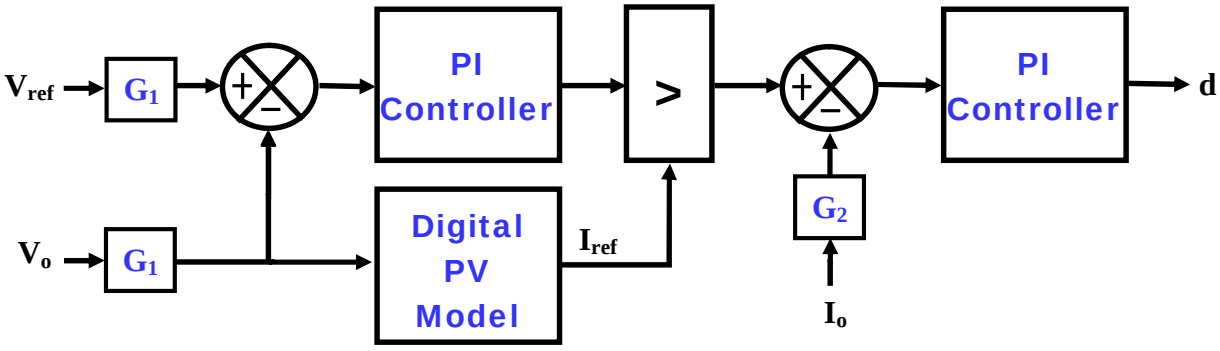

Figure9 Control Block diagram of Solar Array Emulator system (G1=0.01, G2=0.0133)

Thus when operating under no-load condition, in order to obtain the open circuit voltage, voltage control loop becomes dominant as my feedback or output voltage (Vo) exceeds Vref and maintains required duty ratio for corresponding configured Voc. Whereas under loaded condition, current control loop becomes dominant and for a respective voltage drop across the load a new Iref is generated which is then compared to the feedback or output current (Io) to generate the required duty ratio for maintaining the corresponding reference current to make the system act as a current source. Since the whole system is driven from a voltage source thus the net system is said to be Current Controlled Voltage source.

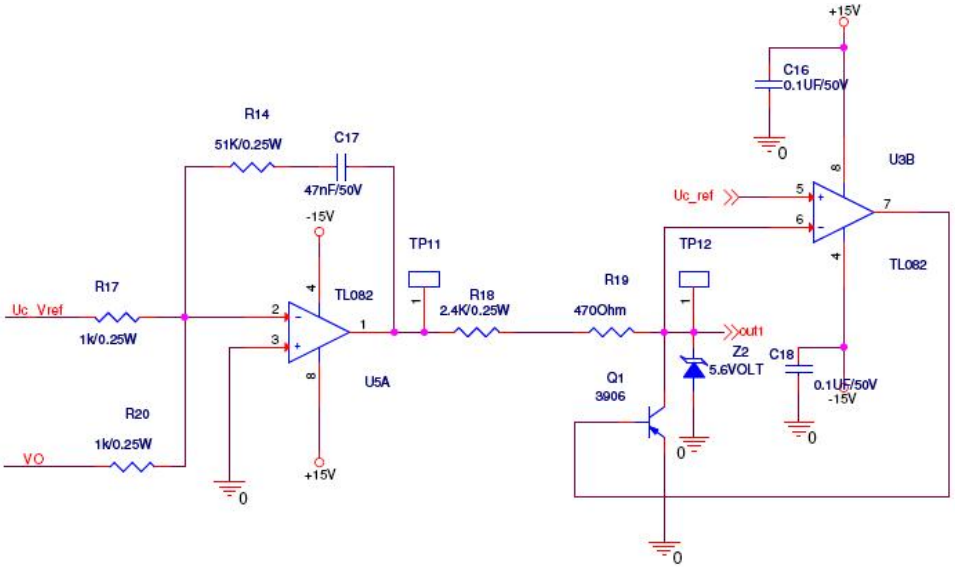

Figure10 PSpice schematic for the mentioned control system

The output (out 1) in the schematic of figure11 is the input to the schematic shown in Figure12 which is compared with the feedback Inductor current of the buck converter through the IC LM3524D to generate the required PWM. This is then fed to the gate driver IC MC33153, responsible for driving the IGBT. Figure 11 shows the PSpice schematic of the implemented control system explained earlier.

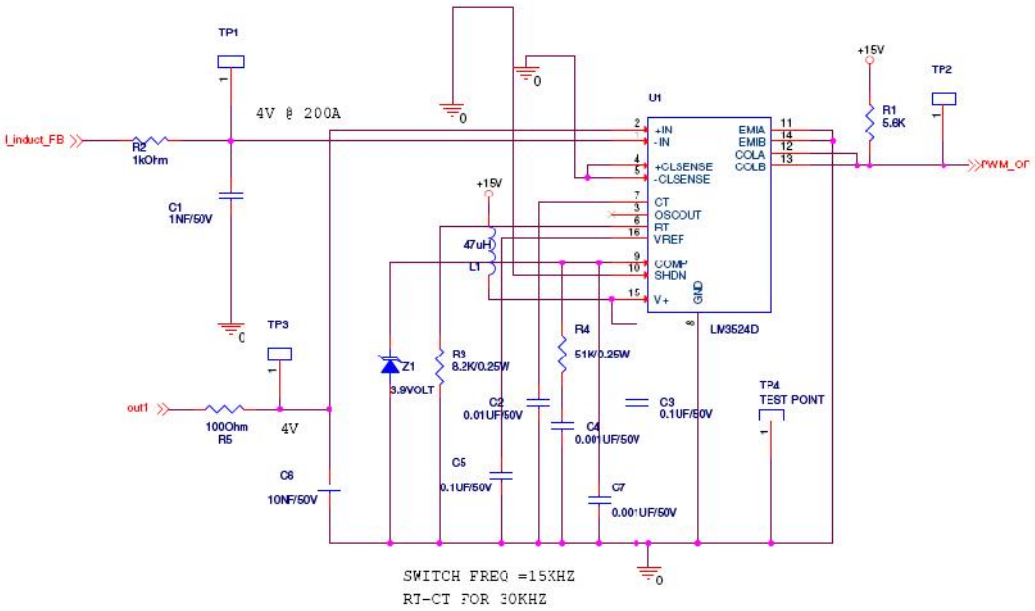

Figure11 PSpice schematic showing generation of PWM through IC LM3524D

4.4 Converter Unit

4.4.1 Buck converter

A Buck converter is a step down converter, produces a average output voltage *Vo* which is lower than the dc input voltage *Vi*, consisting of a switching network of two switches i.e. S1 & S2 as shown in Figure12 whose output is filtered by an LC filter. The basic circuit, in Figure12, constitutes a step down converter for a purely resistive load. The low pass LC-filter, consisting of an inductor and capacitor, very much diminishes the output voltage fluctuations of the switching network. Figure13-a shows waveform of the input voltage V_D (voltage across the diode) to the low pass filter with dc component V_o. In steady-state analysis, filter capacitor at the output is assumed to be very large, as is normally is in the applications requiring a nearly constant instantaneous output voltage $v_o(t) \approx V_o$, We observe that in a step-down converter, average inductor current is equal to the average output current *Io*, since the capacitor current is steady state is zero.

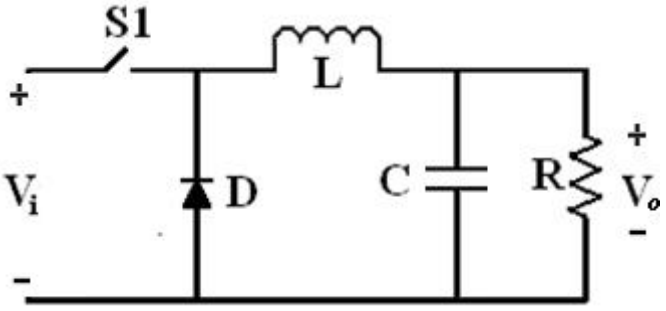

Figure12 Buck Converter with LC filter

We will be confining our discussion to the continuous mode of operation where inductor current flows continuously i.e. $i_L(t)>0$. Related waveforms for the complete cycle is shown in Figure13-a. During the interval when switch is on for a time duration T_{on}, circuit in Figure12 is deduced to the circuit shown in Figure13-b, as the switch conducts diode *D* becomes reverse biased and the input provides energy to the load as well as to the inductor. This results in a positive voltage, $v_L = V_i - V_o$ across the inductor. This voltage causes a linear increase in inductor current i_L. During the interval when the switch is off for a duration T_{off}, circuit in Figure12 is deduced to the circuit shown in Figure13-c, the inductor current flows through the diode, transferring some of its stored energy to the load. When the switch is turned off, because of the inductive energy storage, i_L continues to flow. This current now flows through the diode and $v_L = -V_o$ [35].

Since in steady-state operation the waveform must repeat form one time period to the next, the integral of the inductor voltage v_L over one time period must be zero, where $T_s=T_{on}+T_{off,}$

$$\int_0^{T_S} v_L dt = \int_0^{T_{on}} v_L dt + \int_{T_{on}}^{T_S} v_L dt = 0 \quad (4.2)$$

In Figure12-c, the above equation implies that area A and B must be equal.
Therefore,

$$(V_i - V_o)T_{on} = V_o(T_s - T_{on}) \quad (4.3)$$

Or

$$\frac{V_o}{V_i} = \frac{T_{on}}{T_s} = D \ (Duty\ ratio) \quad (4.4)$$

Therefore, in this mode, the voltage output varies linearly with duty ratio of the switch for a given input voltage. It does not depend on any other circuit parameter. Neglecting the power losses associated with all the circuit elements, the input power Pi equals the output power Po.

$$P_i = P_o \quad (4.5)$$

Therefore,

$$V_i I_i = V_o I_o \quad (4.6)$$

And

$$\frac{I_o}{I_i} = \frac{V_i}{V_o} = \frac{1}{D} \quad (4.7)$$

The output capacitor is assumed to be so large as to yield $v_o(t)=Vo$. However, ripple in output voltage with a practical value of capacitance can be calculated considering the Figure12 in continuous mode of operation. Assuming that all the ripple component in i_L flows through the capacitor and its average component flows through the load resistor, the shaded area in Figure7-e represents an additional charge ΔQ. Therefore, peak -to-peak voltage ripple ΔV_o can be written as

$$\Delta V_o = \frac{\Delta Q}{C} = \frac{1}{C}\frac{1}{2}\frac{\Delta I_L}{2}\frac{T_s}{2} = \frac{\Delta I_L}{8 \times C \times fsw} \quad (4.8)$$

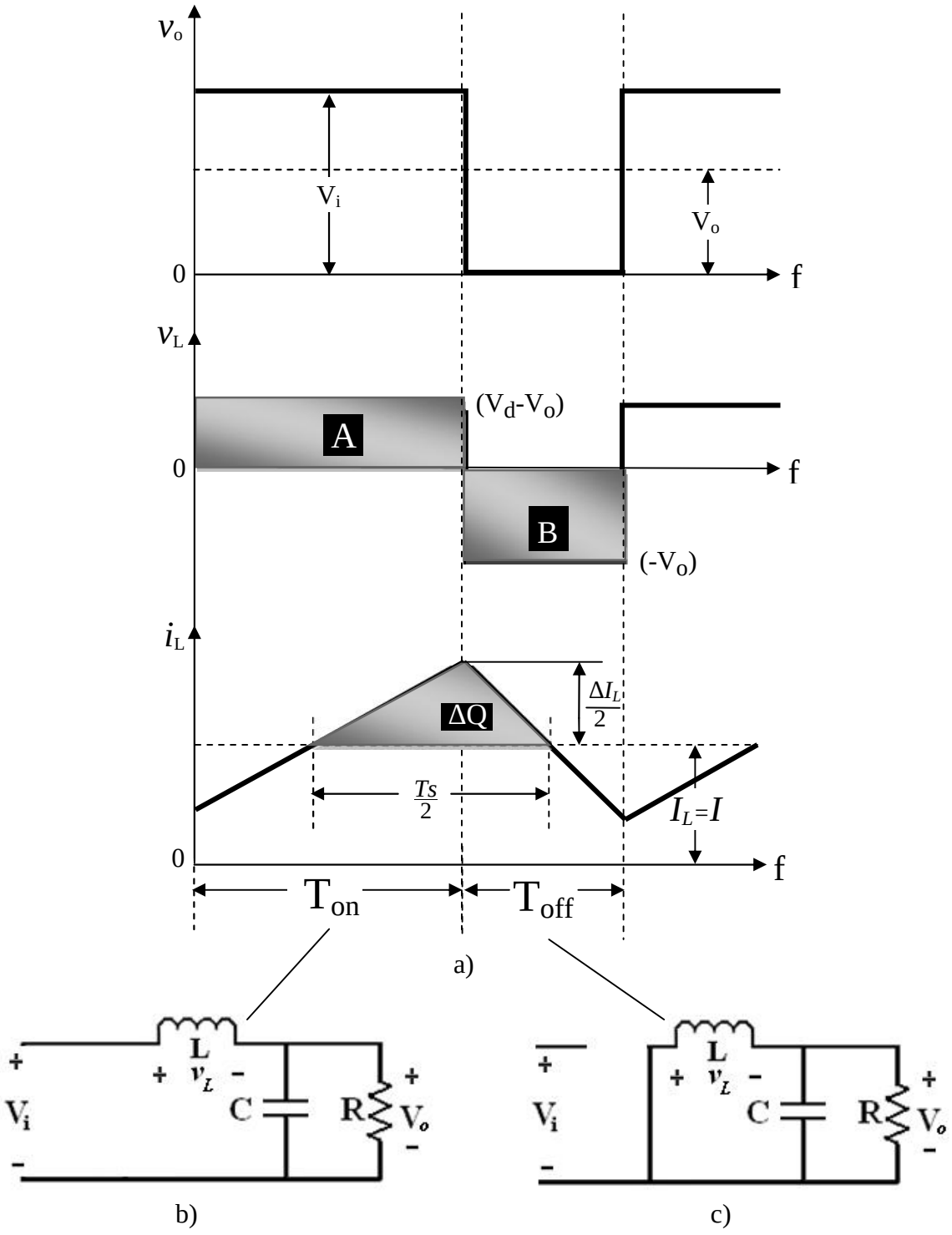

Figure13 Buck converter waveforms and operating modes [36];

a) Waveforms of v_o,v_L,i_L; b) T_{on} mode; c) T_{off} mode.

And during turn off,

$$\Delta I_L = \frac{V_o}{L}(1-D)T_s \tag{4.9}$$

Therefore, substituting ΔI_L from equation 22 into equation 21 giving,

$$\frac{\Delta V}{Vo} = \frac{1}{8}\frac{T_s^2(1-D)}{LC} = \frac{1}{8}(1-D)\left(\frac{f_c}{f_{sw}}\right)^2 \tag{4.10}$$

Where switching frequency $f_{sw} = 1/T_s$ and

$$f_c = \frac{1}{2\Pi\sqrt{LC}} \tag{4.11}$$

Equation 23 shows that the ripple in voltage can be minimized by selecting a corner frequency f_c of the low-pass filter at the output $f_c << f_s$. Also, the ripple is independent of the output load power, so long as the converter operates in the continuous conduction mode. For switch mode power supplies usually the acceptable output voltage ripple is specified, for instance less than 1% in the case of SAE.

A Simulink model for SAE as shown in Figure14 including both the converter unit and the control unit was developed to confirm the feasibility of the concept. And the related simulation results are provided in the next section.

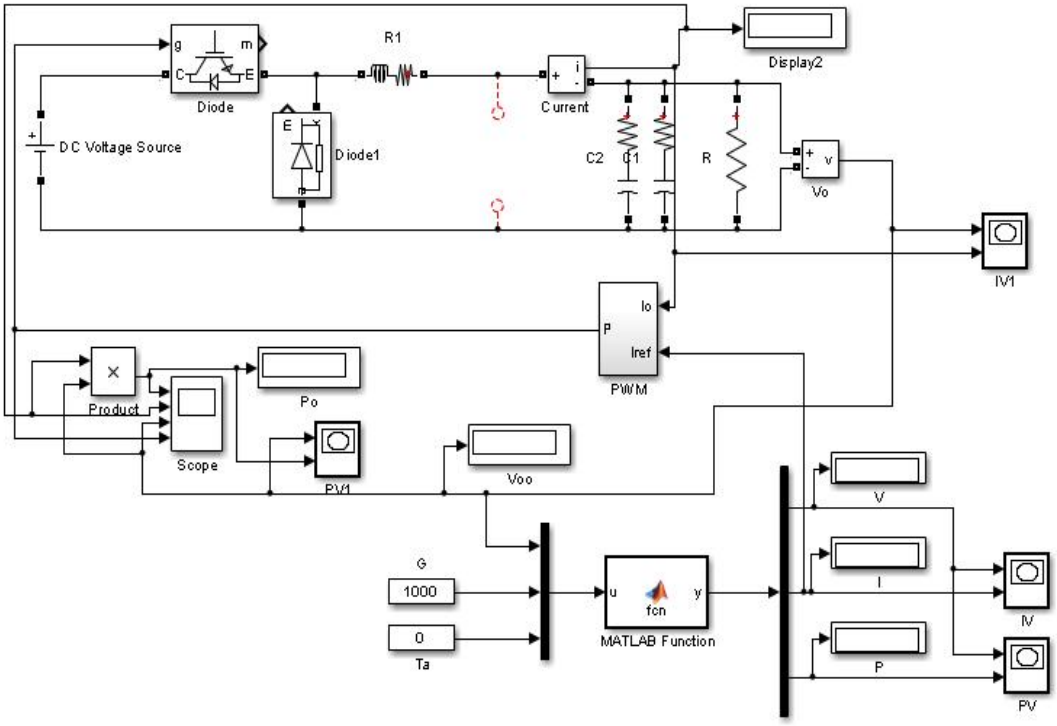

Figure14 Simulink model for SAE including both the control unit and the converter unit.

4.4.2 Design Specifications

Total Load on converter

Total load on SAE

$$P_{out} = PV_{output} = (PanelRating) \times (No.ofPanels)$$
$$PV_{output} = (130W) \times (3 \times 4)$$
$$P_{out} = 1.56kW$$

With an overload factor of 10%, net system rating is 1.7kW.

Input Voltage Range to 3phase Bridge Rectifier

Minimum input voltage from Generator – $V_{rms\,(\min)} = 104Vac$

Maximum input voltage from Generator – $V_{rms\,(\max)} = 202Vac$

DC-DC Converter Efficiency (Rectifier + Buck converter) $\eta = 0.9(Assume)$

Input power of converter = $P_{in} = \frac{P_{out}}{\eta} = \frac{1.7 \times 1000}{0.9} = 1.9kW \approx 2.0kW$

Number of phases = 3

The maximum current through rectifier is considered at 104V.

Per phase input maximum current –

$$I_{rms\_\max} = \frac{P_{in}}{V_{rms\,(\min)} \times \sqrt{3}} = \frac{2.0kW}{104 \times \sqrt{3}} = 11.102\,A$$

Assume for 150% Load –

$$I_{rms(\max@150\%)} = I_{rms(\max)} \times 1.5 = 11.102 \times 1.5 = 16.65A$$

Peak current to for 150% Load –

$$I_{peak(\max@150\%)} = I_{rms(\max@150\%)} \times \sqrt{2} \times 1.1 = 25.9A$$

Thus, Power Bridge Rectifier rating is 415VAC /100A current - 3phase.

Part Number – SKD 100 / 08

As per datasheet included in Appendix B, the maximum V_f (forward voltage) for power loss calculation is 1.35 V.

So per diode loss in the bridge rectifier,

$$P_{lossbridge} = \frac{I_{OUT} \times V_F \times 6}{3} = \frac{11.102 \times 1.35 \times 6}{3} = 29.97W$$

DC Voltage Range to Buck Converter

O/P voltage of Bridge rectifier – $V_{dc(\min)} = \frac{3\sqrt{2} \times V_{rms(\min)}}{®} = \frac{3\sqrt{2} \times 100}{®} \approx 140Vdc$

O/P voltage of Bridge rectifier – $V_{dc(\max)} = \frac{3\sqrt{2} \times V_{rms(\max)}}{®} = \frac{3\sqrt{2} \times 150}{®} \approx 200Vdc$

Nominal output voltage of buck converter – $V_{buck} = 48Vdc$

Minimum expected Voltage ($V_{buck(\max)}$) = $34Vdc$ (Assumed)

Open Circuit Voltage ($V_{buck(\min)}$) = $63Vdc$

Maximum Duty cycle ($D_{\max}$) = $\frac{V_{buck(\max)}}{V_{dc\min}} = \frac{63}{140} = 0.45$

Minimum Duty cycle ($D_{\min}$) = $\frac{V_{buck(\min)}}{V_{dc(\max)}} = \frac{25}{200} = 0.125$

Buck Device Selection

Maximum DC voltage for selection of device,

$$V_{dc(\max)} \times 1.5_{(Assumed)} = 200 \times 1.5 = 300Vdc$$

Peak current, $I_{peak} = \frac{P_{out}}{V_{buck}} = \frac{1.7kW}{48} = 35.42A$

Assume for 150% Load, $I_{peak(\max@150\%)} = 35.42 \times 1.5 = 53.13A$

Buck device selection parameter, Voltage 400Vdc and Current 100A. Thus, IGBT of part number FF400R06KE3 is used. Values for loss calculation are referred from Appendix C.

Freewheeling diode Selection

Dc blocking voltage = $V_{dc\max} \times 1.5_{(Assumed)} = 200 \times 1.5 = 300Vdc$

Average Current in Switch, $I_{avg} = I_{peak} \times (1 - D_{\min})$

$$I_{avg} = 35.42 \times (1 - 0.17) = 29.39A$$

Output Capacitor Calculation/ Selection

Allowable ripple current in the capacitor is assumed as 10% of the load current**.** According to the requirement of an output, similar to that of a PV, should have minimum ripple. Hence in design the ripple voltage is taken as 100mV (assumed).

$$I_{RIPPLE-PKtoPK} = 10\% \times I_{\max} = 10\% \times 35.42 = 3.54A$$

$$C_{OUT} = \frac{I_{RIPPLE-PKtoPK}}{8 \times V_{RIPPLE} \times Fsw} = \frac{3.54}{8 \times 0.15 \times 15000}$$

$$= 300\ uF\ /100\ Vdc$$

But this is not standard value so capacitor value is $300\ uF\ /100\ Vdc$.

Net Capacitor ESR is 213mOhm.

So power losses = $I_{RIPPLE-PKtoPK}{}^2 \times 213m\Omega$

$$= 3.54^2 \times 213m\Omega = 2.67W$$

Input Capacitor Calculation/ Selection

$$C_{IN} = \frac{I_{PEAK} \times Ts}{8 \times V_{RIPPLE}}$$

$$C_{IN} = \frac{16.06 \times 66.67uS}{8 \times 11.5}$$

$$C_{IN} = 116\ uF$$

But this is not standard value, so capacitor value is $120uF\ /450vDC$

Buck Inductor Calculation

Inductor ripple current assumed to be 10% of peak current.

Ripple current,

$$I_{ripple} = I_{peak} \times 0.10 = 35.42 \times 0.10 = 3.54A$$

Ripple peak current in inductor,

$$I_{\text{peak,rp}} = I_{\text{peak}} + (I_{ripple}/2) = 35.42 + (3.54/2) = 37.19A$$

Assuming switching frequency (f_{sw}) =15 kHz

Thus, Inductance,

$$L = \frac{(V_{dc\max} - V_{buck}) \times ((D_{\min})/(fsw))}{I_{ripple}} = \frac{((200-48) \times (0.125/15000))}{3.54} \approx 360uH$$

Power dissipation calculations (at Dmax)

Conduction losses (P_{cond})

$$P_{cond} = V_{CE(SAT)} \times I_{max} \times D_{max}$$

$$P_{cond} = 1.5 \times 35.42 \times 0.45 = 23.9W$$

Conduction losses in diode,

$$P_{condd} = V_F \times I_{Davg} \times (1 - D_{max})$$

$$P_{condd} = 1.3 \times 35.42 \times (1 - 0.45) = 25.33W$$

This calculations is with respect to $V_{GE} = 15V$

Switching Losses in switch,

$$P_{SWM} = (E_{ONM} + E_{OFFM}) \times F_{SW}$$

$$P_{SWM} = (3.2 + 15) \times 1e^{-03} \times 15e^{3}$$

$$= 273W$$

Switching Losses in diode,

$$P_{SWD} = (E_{OND} + E_{OFFD}) \times F_{SW}$$

$$= 7.4 \times 1e^{-03} \times 15e^{3}$$

$$= 111W$$

Total losses in IGBT,

$$P_C = P_{cond} + P_{condd} + P_{SWM} + P_{SWD}$$

$$= 23.9 + 25.33 + 273 + 111$$

$$= 433.23W$$

Total Losses with switching devices and capacitors as follows

$$= 433.23W + 2.67W = 435.9W$$

With respect to Diode Bridge and at D_{MAX} the losses are as follows,

$$= 435.9W + 50W = 485.9W$$

<u>Power dissipation calculations</u> (at D_{min})

Conduction losses (Pcond)

$$P_{cond} = V_{CE(SAT)} \times I_{max} \times D_{min}$$

$$P_{cond} = 1.5 \times 35.42 \times 0.125 = 6.64W$$

Conduction losses in diode

$$P_{condd} = V_F \times I_{davg} \times (1 - D_{min})$$

$$P_{condd} = 1.3 \times 32.42 \times (1 - 0.125) = 36.88W$$

This calculations is with respect to $V_{GE} = 15V$

Switching Losses in switch,

$$P_{SWM} = (E_{ONM} + E_{OFFM}) \times F_{SW}$$

$$P_{SWM} = (3.2 + 15) \times 1e^{-03} \times 15e^{3}$$

$$= 273W$$

Switching Losses in diode,

$$P_{SWD} = (E_{OND} + E_{OFFD}) \times F_{SW}$$

$$= 7.4 \times 1e^{-03} \times 15e^{3}$$

$$= 111W$$

Total losses in IGBT,

$$P_C = P_{cond} + P_{condd} + P_{SWM} + P_{SWD}$$

$$= 6.64 + 36.88 + 273 + 111$$

$$= 427.52W$$

Total Losses with switching devices and capacitors as follows

$$= 427.52W + 2.67W = 430.19W$$

With respect to Diode Bridge and at D_{MIN} the losses are as follows,

$$= 430.19W + 100W = 530.19W$$

4.5 Conclusion

This chapter included a detailed system description with all the necessary calculations. In the subsequent chapter we will be looking at the built prototype and conclude with our results and related discussions for the proposed system.

5 Results & Discussions

5.1 Introduction

This chapter concludes this dissertation with detailed results and discussions along with conclusions and the future scope of work. MATLAB-Simulink simulations of the developed model and scope output of the hardware have been included.

5.2 Simulations

With the use of the developed mathematical Simulink model for 130W WAREE WS-130 desired characteristics were obtained for different Irradiance & Temperature, as shown in Figure15 & 16.

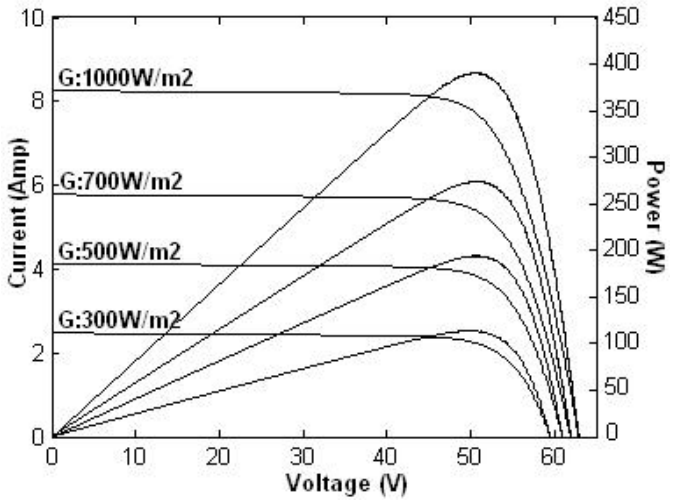

Figure15 Simulated desired Characteristics at different Irradiance

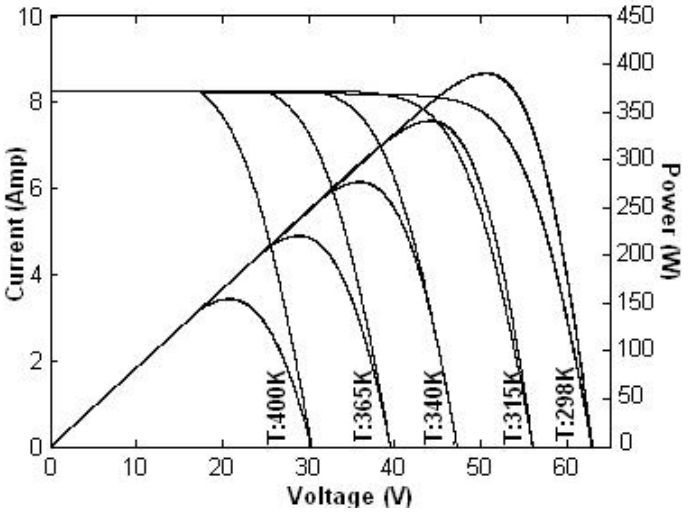

Figure16 Simulated desired Characteristics at different Temperature.

And when the three series connected panels are at different Irradiance level then the corresponding complex characteristics generated are obtained through the model, as shown in Figure17.

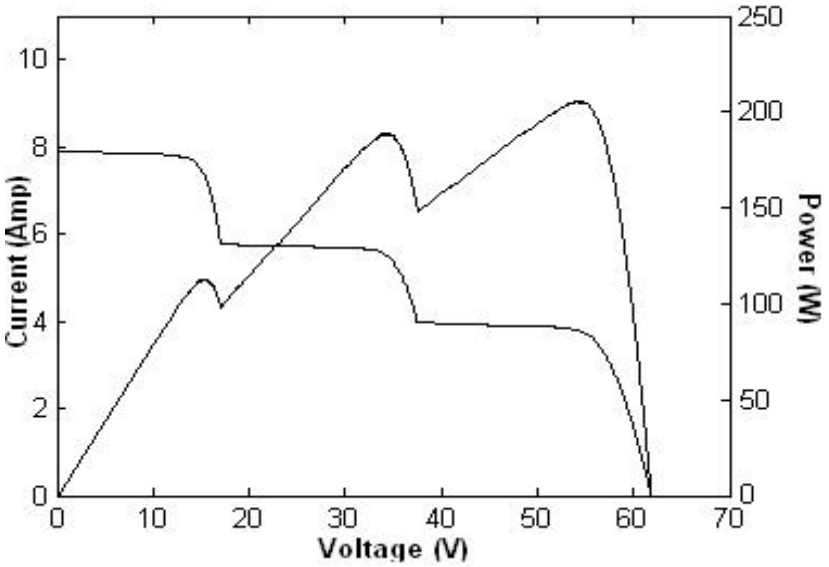

Figure17 Simulated complex characteristics.

SAE implemented through the designed schematic as discussed in the previous section delivers the results in accordance with the simulations.

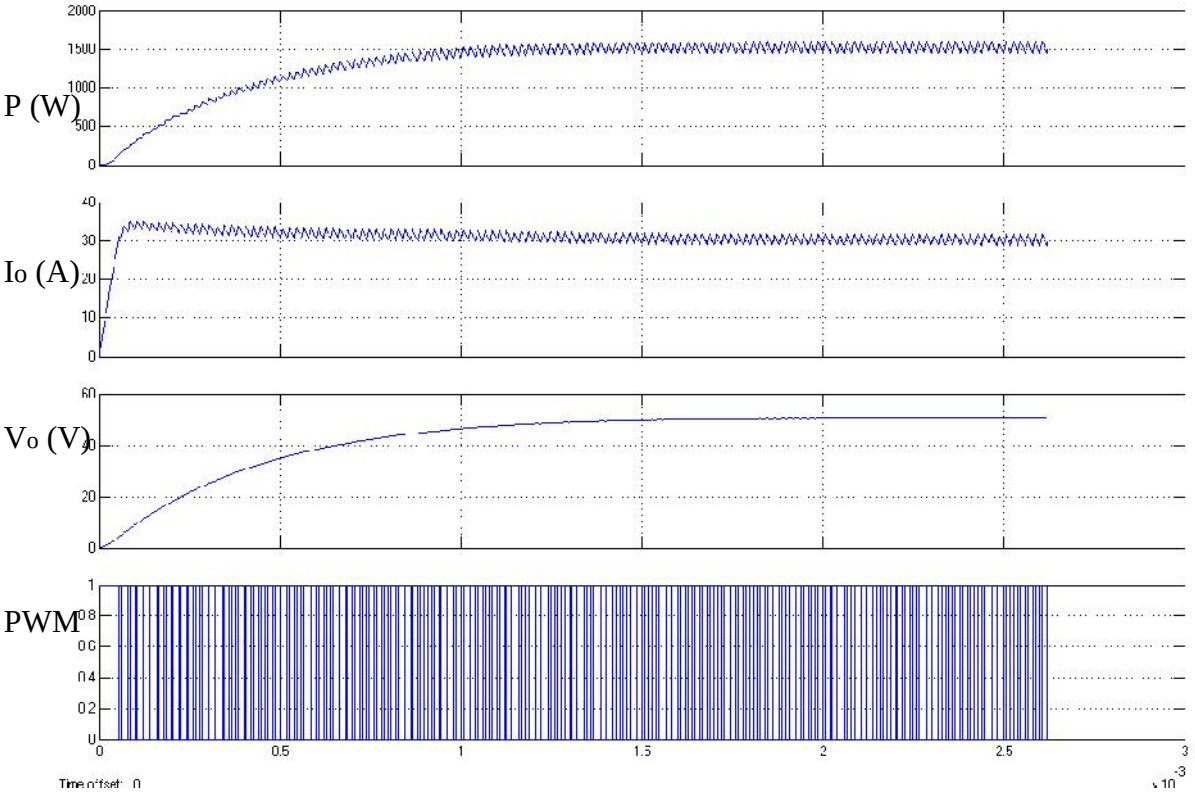

Figure18 Simulation for the Simulink model of SAE.

Change in respect to P, I, V waveforms with respect to PWM pulses is Shown in Figure19. Clearly depicting the current and voltage ripples in the system.

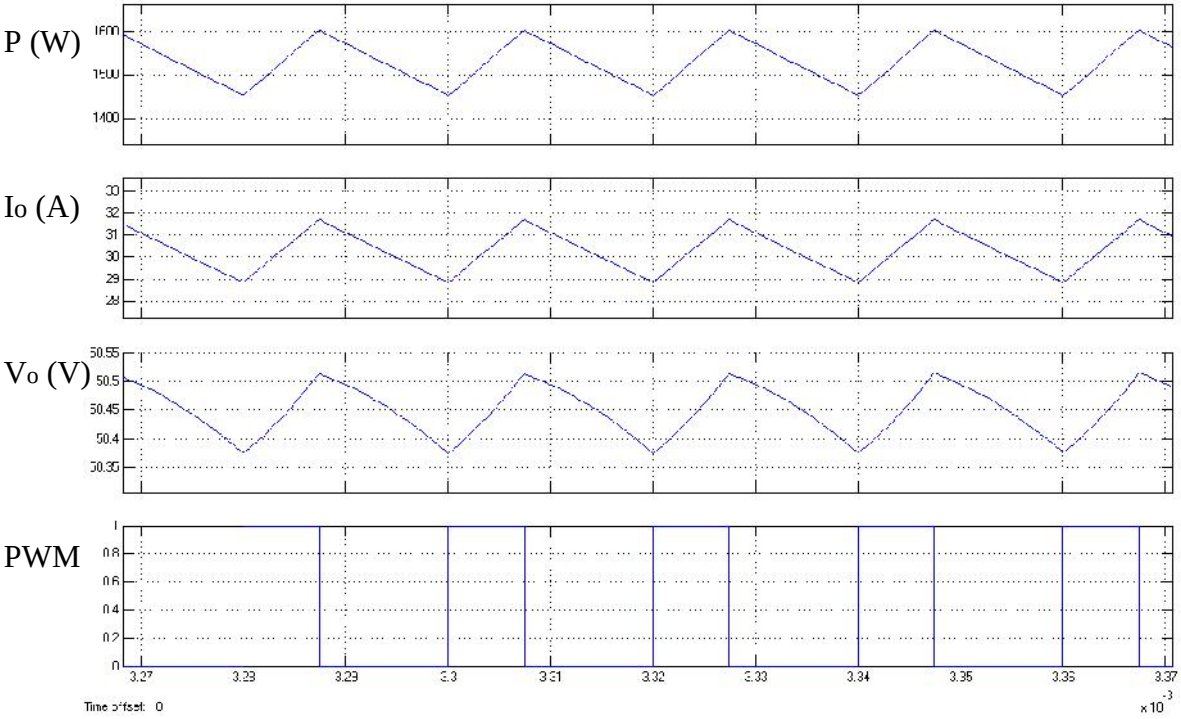

Figure19 Zoomed simulation for the Simulink model of SAE.

5.3 Hardware and Scope Output

Figure20 shows the implemented SAE hardware and Figure21 shows the test facility,where as in the following figures scope ouput of the testing is shown.

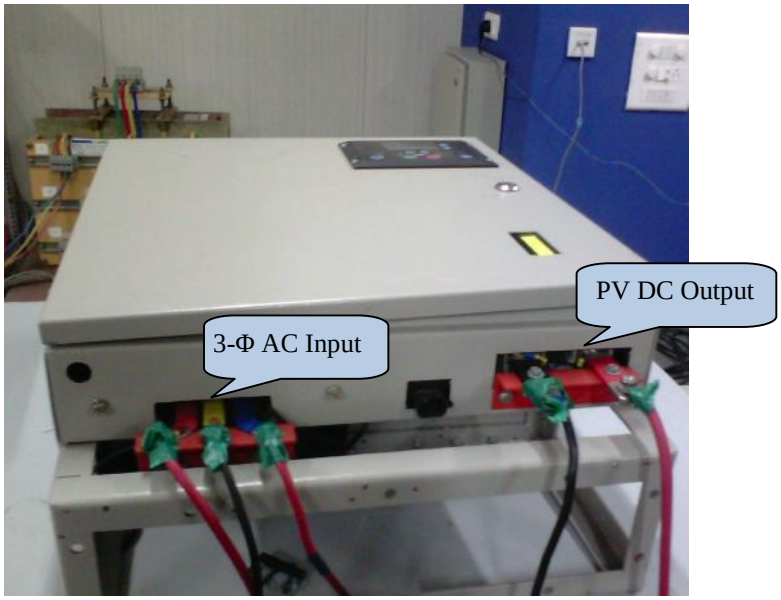

Figure20 SAE Hardware.

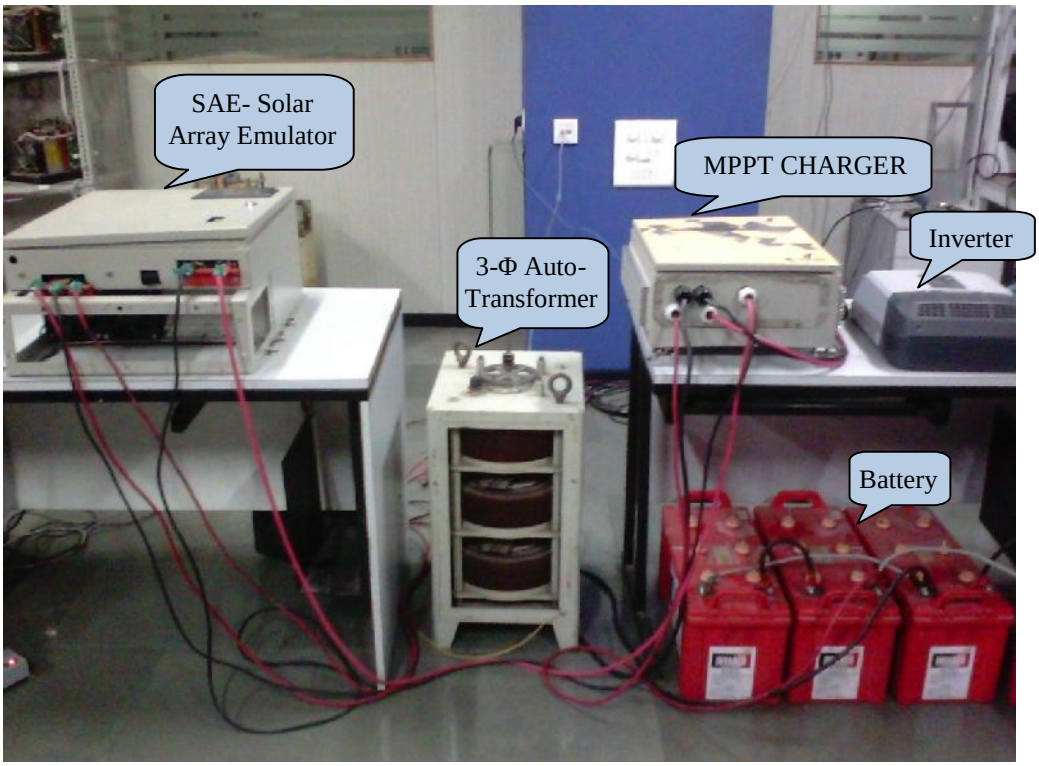

Figure21 SAE Testing Facility.

Figure22 Scope output for Open Circuit Condition.

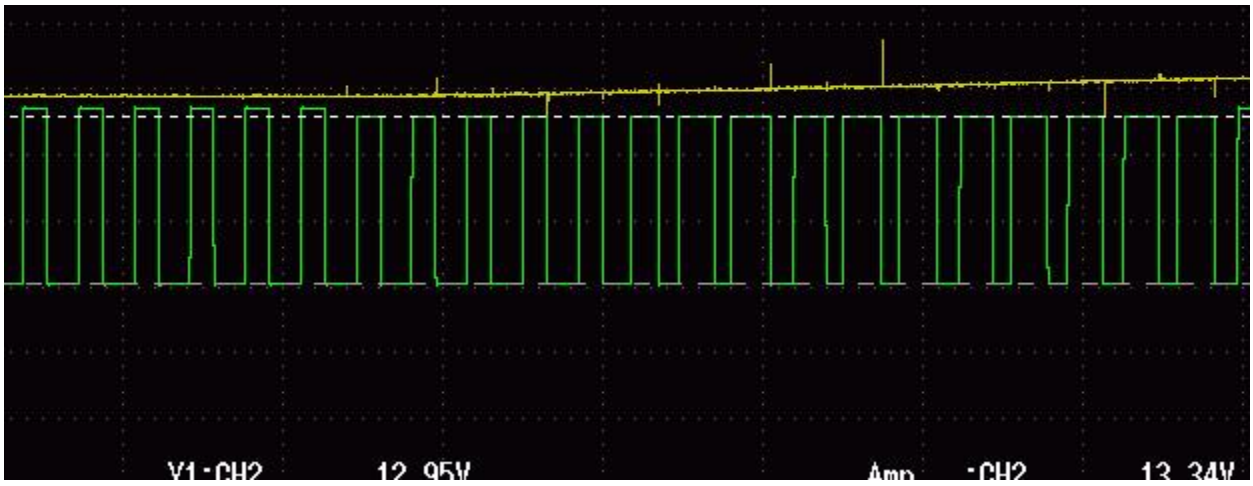

Figure23 Scope output for PWM generated during the Open circuit Voltage Condition.

Figure24 Scope output for change in voltage & current level as soon as the MPPT charger starts tracking depending upon the load condition (CH1: PV Voltage, CH2: PV Current).

Current ripple in the system output can be seen from the Scope output for SAE as shown in Figure25at a load lower than MPP, i.e. 1.4kW which is decided through the wattage of the lamp load bank. Scope output shows both the current (CH3) and voltage (CH1) profile.

Similarly the coltage ripple can also be seen and both comes in accordance with the simulation results.

Figure25 Scope output of SAE at a load demand lower than MPP, i.e. 1.4kW.

A repeated traced scope output of SAE as shown in Figure26 explicitly shows the efficiency and redudancy of the system in delivering the required IV-characteristics inorder to test the DUT. The lower extreme point B show the operating point at which a constant current of approx. 21A at 55V is drawn from the source, i.e. SAE to charge the battery in case of no load. And as we load the source a voltage drop leads to rise in corresponding value of current leading to the tracing of the shown curve. The left most extreme point A in the testing is 43V and 31.2 A showing a drawn power 1.35kW with respect to the connect load. The result can also be seen through the LCD interface as shown in Figure27.

Figure26 Traced Scope output of SAE for different loads.

Figure27 LCD output for the corresponding point A.

Now considering the maximum operating point. DUT draws near about maximum rated power set from SAE. With a obtained MPP point with 49.75V and 30.65A, DUT is drawing a power of 1.53kW from SAE thus giving a near efficacy of 99%. Although there is always some steady state error in the system the estimated efficacy should be marginally more.

Figure28 Scope output displaying MPP.

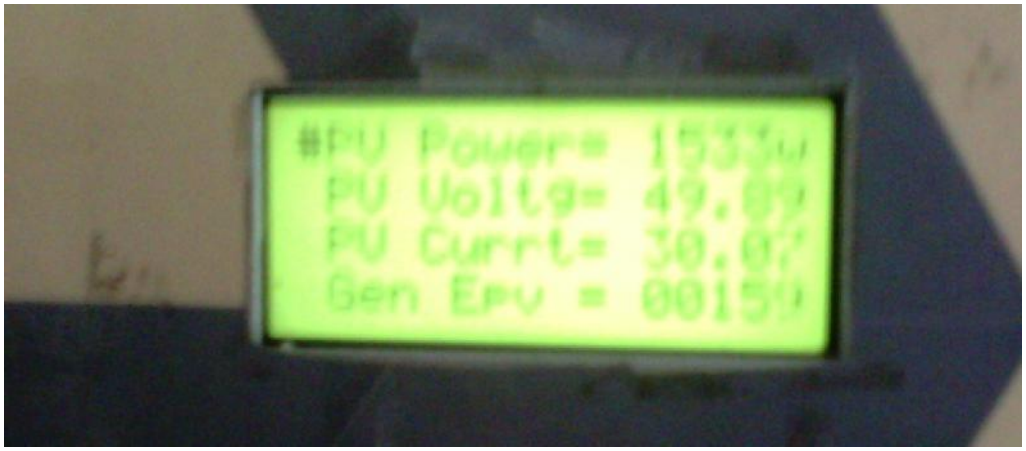

Figure29 LCD output displaying the MPP.

5.4 Conclusion & Future scope of work

The concept behind SAE through a detailed description of various models has been discussed, referring to which a Simulink based PV model has been presented in this dissertation. Various PV array simulation schematic could be created by the proposed model,

and parameters of irradiance and temperature of each PV module model can be set independently. The PV array simulation model allows us to investigate the characteristics of a PV array under various conditions of different irradiance and temperature. Using which, a control method for achieving the PV characteristics through DC-DC buck converter at different irradiance and temperature levels have been proposed and implemented. The work can be extended with the use algorithms to deduce the required solar array parameter parameters for digital implementation of the PV model. Also use of Buck-boost related topology could be implemented to achieve wide ranges of voltage.

Appendix A

WAAREE PV Panel (Ravi Series) Datasheet

WAAREE

WS-120 TO WS-160

TECHNICAL SPECIFICATIONS - WAAREE PV MODULES

Electrical Characteristics *		WS-120/WU-120	WS-125/WU-125	WS-130/WU-130	WS-140/WU-140	WS-150	WS-160
Power (Pm) in Watts (nominal)		120	125	130	140	150	160
Open Circuit Voltage (Voc) in Volts		21	21	21	21	43	43
Short Circuit Current (Isc) in Amps		7.62	7.94	8.25	8.89	4.65	4.96
Voltage at Maximum Power (Vmp) in Volts		17	17	17	17	35	35
Current at Maximum Power (Imp) in Amps		7.06	7.35	7.65	8.24	4.29	4.57
Maximum System Voltage		1000V/600V	1000V/600V	1000V/600V	1000V/600V	1000V	1000V
Physical Parameters (Refer drawing below)							
Solar Cells per Module (Units)		36	36	36	36	72	72
Length x Width x Thickness (L x W x T)	mm(Inches)	1490 x 675 x 35 (58.7 x 26.6 x 1.4)				1175 x 990 x 35(46.3 x 39.0 x 1.4)	
Weight - Kg		11.75	11.75	11.75	11.75	14.45	14.45
Mounting Holes Pitch (Y)	mm(Inches)	915(36.0)				595(23.4)	
Mounting Holes Pitch (X)	mm(Inches)	627(24.7)				945(37.2)	
Area - Sq. M / Area - Sq. ft.		1.009(10.86)				1.163(12.52)	
Junction Box		IP 65 with Diodes	IP 65 with Diodes	IP 65 with Diodes	IP 65 with Diodes	IP 65 with Diodes	IP 65 with Diodes

*Measurement Tolerance on Power +/- 5%. All electrical parameters specified at STC : 25°C cell temperature; 100mW/cm² irradiance; AM 1.5

Other Characteristics

Type of Cell	:	Mono / Multi Crystalline Silicon
Front Face	:	Tempered Glass (Low Iron)
Encapsulate	:	Ethylene Vinyl Acetate
Frame	:	Anodized Aluminium
Junction Box	:	Weather Proof Nylon 6
Temp. Coefficients	:	Voltage -0.123 V / °K Current +4.4 mA / °K Power -0.47% / °K
NOCT	:	47+/-2 °C

- Certifications: IEC 61215 / IEC 61730 -1 / IEC 61730 – 2 / TUV Safety Class II & ETL Mark for UL 1703 approval (USA & CANADA); CEC listed
- The Standard range of modules is supplied without diodes. However, diodes can be provided on specific customer request at extra cost.
- All modules are supplied with screwless Hollow section frames.
- Warranty : Up to 25 Years Limited Extended Warranty
- Due to constant product modifications, WAAREE reserves the right to amend the above specifications without prior notice.

Mounting Details

All dimensions in mm and tolerances ±2mm

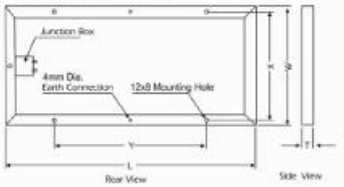

WAAREE Energies Pvt. Ltd.

HO - Mumbai India
Tel- +91 (022) 66444444
Factory - Surat India
Fax - +91 (022) 6644 4400
Email : waaree@waaree.com

Sun Power Forever

www.waaree.com

Appendix B

Power Bridge Rectifier (SKD 100/08) Datasheet

SKD 100

SEMIPONT® 2

Power Bridge Rectifiers

SKD 100

Features

- Robust plastic case with screw terminals
- Large, isolated base plate
- Blocking voltage to 1600 V
- High surge currents
- Three phase bridge rectifier
- Easy chassis mounting
- UL recognized, file no. E 63 532

Typical Applications*

- Three phase rectifiers for power supplies
- Input rectifiers for variable frequency drives
- Rectifiers for DC motor field supplies
- Battery charger rectifiers

1) Painted metal sheet of minimum 250 x 250 x 1 mm: $Rh_{th(c-a)}$ = 1,8 K/W

V_{RSM} V	V_{RRM}, V_{DRM} V	I_D = 100 A (full conduction) (T_c = 93 °C)
400	400	SKD 100/04
800	800	SKD 100/08
1200	1200	SKD 100/12
1400	1400	SKD 100/14
1600	1600	SKD 100/16

Symbol	Conditions	Values	Units
I_D	T_c = 85 °C	110	A
	inductive load		A
	T_a = 45 °C, chassis 1)	24	A
	T_a = 45 °C; P13A/125 (P1A/120)	28 (54)	A
	T_a = 35 °C, P1A/120F (P1A/200F)	100 (120)	A
I_{FSM}	T_{vj} = 25 °C; 10 ms	1150	A
	T_{vj} = 125 °C; 10 ms	1000	A
i^2t	T_{vj} = 25 °C; 8,3 ... 10 ms	6600	A²s
	T_{vj} = 125 °C; 8,3 ... 10 ms	5000	A²s
V_F	T_{vj} = 25 °C; I_F = 150 A	max. 1,35	V
$V_{(TO)}$	T_{vj} = 125 °C	max. 0,85	V
r_T	T_{vj} = 125 °C	max. 5	mΩ
I_{RD}	T_{vj} = 25 °C; V_{DD} = V_{DRM}; V_{RD} = V_{RRM}	max. 0,5	mA
	T_{vj} = 125 °C, V_{RD} = V_{RRM}	2	mA
$R_{th(j-c)}$	per diode	0,85	K/W
	total	0,14	K/W
$R_{th(c-s)}$	total	0,05	K/W
T_{vj}		- 40 ... + 125	°C
T_{stg}		- 40 ... + 125	°C
V_{isol}	a. c. 50 Hz; r.m.s.; 1 s / 1 min.	3600 (3000)	V
M_s	to heatsink	5 ± 15 %	Nm
M_t	to terminals	5 ± 15 %	Nm
m		165	g
Case		G 18	

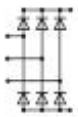

SKD

Appendix C

IGBT Module (FF400R06KE3) Datasheet

Technische Information / Technical Information

IGBT-Module
IGBT-modules

FF400R06KE3

62mm C-Serien Modul mit Trench/Feldstop IGBT3 und Emitter Controlled3 Diode
62mm C-Serien module with trench/fieldstop IGBT3 and Emitter Controlled3 diode

IGBT,Wechselrichter / IGBT,Inverter

Höchstzulässige Werte / Maximum Rated Values

Kollektor-Emitter-Sperrspannung Collector-emitter voltage	T_{vj} = 25°C	V_{CES}		600	V
Kollektor-Dauergleichstrom Continuous DC collector current	T_C = 70°C, $T_{vj\,max}$ = 175°C T_C = 25°C, $T_{vj\,max}$ = 175°C	$I_{C\,nom}$ I_C		400 500	A A
Periodischer Kollektor-Spitzenstrom Repetitive peak collector current	t_P = 1 ms	I_{CRM}		800	A
Gesamt-Verlustleistung Total power dissipation	T_C = 25°C, $T_{vj\,max}$ = 175	P_{tot}		1250	W
Gate-Emitter-Spitzenspannung Gate-emitter peak voltage		V_{GES}		+/-20	V

Charakteristische Werte / Characteristic Values

			min.	typ.	max.	
Kollektor-Emitter-Sättigungsspannung Collector-emitter saturation voltage	I_C = 400 A, V_{GE} = 15 V I_C = 400 A, V_{GE} = 15 V I_C = 400 A, V_{GE} = 15 V	T_{vj} = 25°C T_{vj} = 125°C T_{vj} = 150°C	$V_{CE\,sat}$	1,45 1,60 1,70	1,90	V V V
Gate-Schwellenspannung Gate threshold voltage	I_C = 6,40 mA, V_{CE} = V_{GE}, T_{vj} = 25°C		$V_{GE(th)}$	4,9	5,8	6,5	V
Gateladung Gate charge	V_{GE} = -15 V ... +15 V		Q_G		4,30		µC
Interner Gatewiderstand Internal gate resistor	T_{vj} = 25°C		R_{Gint}		1,0		Ω
Eingangskapazität Input capacitance	f = 1 MHz, T_{vj} = 25°C, V_{CE} = 25 V, V_{GE} = 0 V		C_{ies}		26,0		nF
Rückwirkungskapazität Reverse transfer capacitance	f = 1 MHz, T_{vj} = 25°C, V_{CE} = 25 V, V_{GE} = 0 V		C_{res}		0,76		nF
Kollektor-Emitter-Reststrom Collector-emitter cut-off current	V_{CE} = 600 V, V_{GE} = 0 V, T_{vj} = 25°C		I_{CES}			5,0	mA
Gate-Emitter-Reststrom Gate-emitter leakage current	V_{CE} = 0 V, V_{GE} = 20 V, T_{vj} = 25°C		I_{GES}			400	nA
Einschaltverzögerungszeit, induktive Last Turn-on delay time, inductive load	I_C = 400 A, V_{CE} = 300 V V_{GE} = ±15 V R_{Gon} = 1,5 Ω	T_{vj} = 25°C T_{vj} = 125°C T_{vj} = 150°C	$t_{d\,on}$		0,11 0,12 0,13		µs µs µs
Anstiegszeit, induktive Last Rise time, inductive load	I_C = 400 A, V_{CE} = 300 V V_{GE} = ±15 V R_{Gon} = 1,5 Ω	T_{vj} = 25°C T_{vj} = 125°C T_{vj} = 150°C	t_r		0,05 0,06 0,06		µs µs µs
Abschaltverzögerungszeit, induktive Last Turn-off delay time, inductive load	I_C = 400 A, V_{CE} = 300 V V_{GE} = ±15 V R_{Goff} = 1,5 Ω	T_{vj} = 25°C T_{vj} = 125°C T_{vj} = 150°C	$t_{d\,off}$		0,49 0,52 0,53		µs µs µs
Fallzeit, induktive Last Fall time, inductive load	I_C = 400 A, V_{CE} = 300 V V_{GE} = ±15 V R_{Goff} = 1,5 Ω	T_{vj} = 25°C T_{vj} = 125°C T_{vj} = 150°C	t_f		0,05 0,07 0,07		µs µs µs
Einschaltverlustenergie pro Puls Turn-on energy loss per pulse	I_C = 400 A, V_{CE} = 300 V, L_S = 30 nH V_{GE} = ±15 V, di/dt = 7000 A/µs (T_{vj} = 150°C) R_{Gon} = 1,5 Ω	T_{vj} = 25°C T_{vj} = 125°C T_{vj} = 150°C	E_{on}		3,20 3,40		mJ mJ mJ
Abschaltverlustenergie pro Puls Turn-off energy loss per pulse	I_C = 400 A, V_{CE} = 300 V, L_S = 30 nH V_{GE} = ±15 V, du/dt = 4500 V/µs (T_{vj} = 150°C) R_{Goff} = 1,5 Ω	T_{vj} = 25°C T_{vj} = 125°C T_{vj} = 150°C	E_{off}		15,0 15,5		mJ mJ mJ
Kurzschlußverhalten SC data	V_{GE} ≤ 15 V, V_{CC} = 360 V V_{CEmax} = V_{CES} -L_{sCE} ·di/dt	t_P ≤ 8 µs, T_{vj} = 25°C t_P ≤ 6 µs, T_{vj} = 150°C	I_{SC}		2800 2000		A A
Wärmewiderstand, Chip bis Gehäuse Thermal resistance, junction to case	pro IGBT / per IGBT		R_{thJC}			0,12	K/W
Wärmewiderstand, Gehäuse bis Kühlkörper Thermal resistance, case to heatsink	pro IGBT / per IGBT λ_{Paste} = 1 W/(m·K) / λ_{grease} = 1 W/(m·K)		R_{thCH}		0,03		K/W
Temperatur im Schaltbetrieb Temperature under switching conditions			$T_{vj\,op}$	-40		150	°C

prepared by: MK	date of publication: 2013-10-03
approved by: WR	revision: 3.0

Appendix D

List of Publications

1. Munjal A., Ganguli S., Wachasundar S., “A simplistic approach to PV Emulator,” International Conference on Energy Efficient LED Lighting & Solar Photovoltaic Systems, IIT Kanpur & IETE, March’2014.
2. Munjal A., “Understanding Solar Power Generation through PV Emulator,” Present Around The World, IET (UK), April’2014.

Appendix E

Patent Recognition from Crompton Greaves Ltd.

Thank You!

Ayush Munjal

I recognize your technology innovation to develop

Understanding Solar Power Generation through PV Emulator

Looking forward to your continued contribution to

IP Movement

Dileep S. Patil

Executive Vice President &
Chief Technology Officer

AVANTHA
GROUP COMPANY

REFERENCES

[1] Salas V., Olías E., Barrado A., Lázaro A., "Review of the maximum power point tracking algorithms for standalone photovoltaic systems," *Solar Energy Materials and Solar Cells*, Vol. 90, Issue 11, pp.1555-1578, July 2006.

[2] Paraskevadaki E.V., Papathanassiou S.A., "Evaluation of MPP Voltage and Power of mc-Si PV Modules in Partial Shading Conditions," *IEEE Trans on Energy Conversion*, vol. 26, pp. 923 – 932, 2011.

[3] Abdelaziz E.A., Saidur R,. Mekhilef S., "A review on energy saving strategies in industrial sector," *Renewable and Sustainable Energy Reviews*, Volume 15, Issue 1, pp. 150-168, Jan. 2011.

[4] Renewable energy in India, MNES report, Government of India, 2001.

[5] Survey of renewable energy in India. TERI (Tata Energy Research Institute), New Delhi; 2001.

[6] Mission Document, Jawaharlal Nehru National Solar Mission, MNRE, 2008. [Online] Available: http://www.mnre.gov.in/solar-mission/jnnsm

[7] Ravi Series WS 120 - WS 160, WAAREE PV Modules specification. [Online] Available: http://www.waaree.com/WaareeDownloadCenter.aspx

[8] Updated India Solar Resource Maps, NREL. [Online] Available: http://www.nrel.gov/international/ra_india.html

[9] Luque A., Hegedus S., Handbook of Photovoltaic Science and Engineering, John Wiley and Sons, 2nd edition, 2003. ISBN 0-471-49196-9.

[10] Patel H., Agarwal V., "MATLAB-based modeling to study the effects of partial shading on PV array characteristics," *IEEE Transactions Energy Conversion*, vol. 23, no. 1, pp. 302–310, Mar. 2008.

[11] Karatepe E., Boztepe M., Metin, C., "Development of a suitable model for characterizing photovoltaic arrays with shaded solar cells," *Solar Energy*, vol. 81, pp. 977–992, 2007.

[12] Vokas G.A., MacHias A.V., Souflis, J.L., "Computer modeling and parameters estimation for solar cells," *IEEE Electrotechnical Conference proceedings*, vol.1, pp. 206-209, May 1991.

[13] Lloyd S.H., Smith G.A., Infield D.G., Lloyd S.H., Smith G.A., Infield, D.G., "Design and construction of a modular electronic photovoltaic simulator," *8th International Conference on Power Electronics and Variable Speed Drives*, pp. 120-123, 2000.

[14] Veerachary M., Senjyu T., Uezato K., "Voltage-based maximum power point tracking control of PV system," *IEEE Transactions on Aerospace and Electronic Systems*, vol. 38, no. 1, pp. 262-270, 2002.

[15] Veerachary M., "PSIM circuit-oriented simulator model for the nonlinear photovoltaic sources," *IEEE Transactions on Aerospace and Electronic Systems*, Vol. 42, Issue: 2, pp. 735 – 740, Apr. 2006.

[16] Sera D., Teodorescu R. , Rodriguez P., "PV panel model based on data sheet values,' *IEEE International Symposium on Industrial Electronics*, pp. 2392-2396, June 2007.

[17] Midtgard O. M., "A simple photovoltaic simulator for testing of power electronics," *Power Electronics and Applications, European Conference*, pp. 1-10, Sept 2007.

[18] Cirrincione M., Di Piazza M.C., Marsala G., Pucci M., Vitale, G., "Real time simulation of renewable sources by model-based control of DC/DC converters," *IEEE International Symposium on Industrial Electronics*, pp. 1548–1555, July 2008.

[19] Yuan Li, Taewon Lee, Peng F.Z., Dichen Liu, "A Hybrid Control Strategy for Photovoltaic Simulator," *24th Annual IEEE Applied Power Electronics Conference and Exposition*, pp. 899 – 903, Feb. 2009.

[20] Koran A., Sano K., Rae-young Kim, Jih-Sheng Lai, "Design of a photovoltaic simulator with a novel reference signal generator and two-stage LC output filter," *IEEE Energy Conversion Congress and Exposition*, pp. 319 – 326, Sep. 2009.

[21] Hengsi Qin, Kimball J.W., "Parameter determination of Photovoltaic Cells from field testing data using particle swarm optimization," *IEEE Power and Energy Conference*, pp. 1-4, Feb. 2011.

[22] Wandhare, R. G.; Agarwal, V., "A low cost, light weight and accurate photovoltaic emulator," *37th IEEE Photovoltaic Specialists Conference*, pp. 1887-1892, 2011.

[23] Ickilli D., Can H., Parlak K.S., "Development of a FPGA-based photovoltaic panel emulator based on a DC/DC converter", *38th IEEE Photovoltaic Specialists Conference*, pp. 1417-1421, June 2012.

[24] Bhise K., Pragallapati N., Thale S., Agarwal V., "LabVIEW based emulation of Photovoltaic array to study maximum power point tracking algorithms," *38thIEEE Photovoltaic Specialists Conference*, pp. 2961–2966, June 2012.

[25] Dylan D.C. Lu, Quang Ngoc Nguyen," A photovoltaic panel emulator using a buck-boost DC/DC converter and a low cost micro-controller," *Solar Energy*, vol. 86, pp. 1477–1484, 2012.

[26] Cheng-Chuan Chen, Hong-Chan Chang, Cheng-Chien Kuo, Chien-Chin Lin, "Programmable energy source emulator for photovoltaic panels considering partial shadow effect," *Energy*, vol. 54, pp. 174-183, 2013.

[27] Kim Y., Lee W., Pedram M., Chang N., "Dual-mode power regulator for photovoltaic module emulation," *Applied. Energy*, vol. 101, pp. 730–739, 2013.

[28] Ishaque K., Salam Z., Taheri H., "Simple, fast and accurate two-diode model for photovoltaic modules," *Solar Energy Mater. Solar Cells*, vol. 95, no. 2, pp. 586–594, Feb. 2011.

[29] Sandrolini L., Artioli M., Reggiani U., "Numerical method for the extraction of photovoltaic module double-diode model parameters through cluster analysis," *Applied. Energy*, vol. 87, no. 2, pp. 442–451, 2010.

[30] Kim W., Choi W., "A novel parameter extraction method for the one diode solar cell model," *Solar Energy*, vol. 84, no. 6, pp. 1008–1019, June 2010.

[31] Soto W. D., Klein S. A., Beckman W. A., "Improvement and validation of a model for photovoltaic array performance," *Solar Energy*, vol. 80, no. 1, pp. 78–88, Jan. 2006.

[32] Ramaprabha R., Mathur B. L., "MATLAB based modelling to study the influence c shading on series connected SPVA," in *Proc. Int. Conf. Emerging Trends Eng. Technol.*, pp.30–34, 2009.

[33] Petrone G., Spagnuolo G., Vitelli M., “Analytical model of mismatched photovoltaic fields by means of Lambert W-function,” *Solar Energy Mater. Solar Cells*, vol. 91, pp. 1652–1657, Nov. 2007.

[34] Ropp M. E., Gonzalez S., “Development of a MATLAB/Simulink model of a single-phase grid-connected photovoltaic system,” *IEEE Transactions Energy Conversion*, vol. 24, no. 1, pp. 195–202, Mar. 2009.

[35] Jiang Y., Qahouq J. A. A., Batarseh I., “Improved solar PV cell MATLAB simulation model and comparison,” *in Proc. IEEE Int. Symp. Circuits Syst.*, pp. 2770–2773, May/June 2010.

[36] Mohan N., Undeland T. M., Robbins W. P., “Power Electronics: Converters, Applications, and Design,” John Wiley & Sons, 3rd edition, 2002.

[37] Veerachary M., Shinoy K.S., “V2-based power tracking for nonlinear PV sources,” *IEEE Proceedings-Electric Power Applications*, vol. 152, no. 5, pp. 126-127, 2005.

,